Global Change Biology (2005) **11,** 1065–1093, doi: 10.1111/j.1365-2486.2005.00971.x

Pan-European $\delta^{13}C$ values of air and organic matter from forest ecosystems

DEBORAH HEMMING*[1], DAN YAKIR*, PER AMBUS†, MIKA AURELA‡, CATHY BESSON§, KEVIN BLACK¶, NINA BUCHMANN‖**, REGIS BURLETT††, ALESSANDRO CESCATTI‡‡, ROBERT CLEMENT§§, PATRICK GROSS¶¶, ANDRÉ GRANIER¶¶, THOMAS GRÜNWALD‖‖, KATARINA HAVRANKOVA***, DALIBOR JANOUS***, IVAN A. JANSSENS†††, ALEXANDER KNOHL‖, BARBARA K ÖSTNER‖‖, ANDREW KOWALSKI††, TUOMAS LAURILA‡, CATARINA MATA‡‡‡, BARBARA MARCOLLA‡‡, GIORGIO MATTEUCCI§§§¶¶¶, JOHN MONCRIEFF§§, EDDY J. MOORS‖‖‖, BRUCE OSBORNE¶, JOÃO SANTOS PEREIRA§, MARI PIHLATIE****, KIM PILEGAARD†, FRANCESCA PONTI††††, ZUZANA ROSOVA***, FEDERICA ROSSI‡‡‡‡, ANDREA SCARTAZZA‡‡‡ and TIMO VESALA****

**Department of Environmental Sciences and Energy Research, Weizmann Institute of Science, 76100 Rehovot, Israel, †Plant Research Department, Risø National Laboratory, Frederiksborgvej 399, PO Box 49, DK-4000 Roskilde, Denmark, ‡Finnish Meteorological Institute, Climate and Global Change Research, Sahaajankatu 20 E, FIN-00880 Helsinki, Finland, §Instituto Superior de Agronomia, Tapada da Ajuda, 1349-017 Lisboa, Portugal, ¶Department of Botany, University College Dublin, Belfield, Dublin 4, Ireland, ‖Max Plank Institute for Biochemistry, PO Box 100164, 07701 Jena, Germany, **Institute of Plant Sciences, Universitätsstrasse 2, ETH Zentrum LFW C56, CH-8092 Zuerich, Switzerland, ††INRA Bordeaux, 33610 Gazinet-Cestas, France, ‡‡Centro di Ecologia Alpina, Viote del Monte Bondone, 38040 Trento, Italy, §§School of GeoSciences, University of Edinburgh, EH9 3JU Edinburgh, UK, ¶¶UMR INRA-UHP Ecologie et Ecophysiologie Forestières, F54280 Champenoux, France, ‖‖Department of Meteorology, Institute of Hydrology and Meteorology, TU Dresden, D-01062 Dresden, Germany, ***Institute of Landscape Ecology, Academy of Sciences of the Czech. Republic, Porici 3B, Brno 603 00, Czech Republic, †††Department of Biology, Universiteitsplein 1, B-2610. Antwerp, Belgium, ‡‡‡CNR, Istituto di Biologia Agroambientale e Forestale, 05010 Porano (TR), Italy, §§§Joint Research Centre, Institute for Environment and Sustainability – IES, Climate Change Unit, T.P. 051, 21020 Ispra (VA), Italy, ¶¶¶Department of Forest Environment and Resources (DISAFRI), University of Tuscia, Via San Camillo de Lellis snc, 01100 Viterbo, Italy, ‖‖‖Alterra, PO Box 47. 6700 AA Wageningen, The Netherlands, ****Department of Physical Sciences, University of Helsinki, P O Box 64, FIN-00014.Helsinki, Finland, ††††Dipartimento di Colture Arboree, Università di Bologna, Via Fanin 46, 40127 Bologna, Italy, ‡‡‡‡Istituto di Biometeorologia, CNR, Via P.Gobetti 101, 40129 Bologna, Italy*

Abstract

We present carbon stable isotope, $\delta^{13}C$, results from air and organic matter samples collected during 98 individual field campaigns across a network of Carboeuroflux forest sites in 2001 (14 sites) and 2002 (16 sites). Using these data, we tested the hypothesis that $\delta^{13}C$ values derived from large-scale atmospheric measurements and models, which are routinely used to partition carbon fluxes between land and ocean, and potentially between respiration and photosynthesis on land, are consistent with directly measured ecosystem-scale $\delta^{13}C$ values. In this framework, we also tested the potential of $\delta^{13}C$ in canopy air and plant organic matter to record regional-scale ecophysiological patterns.

Our network estimates for the mean $\delta^{13}C$ of ecosystem respired CO_2 and the related 'discrimination' of ecosystem respiration, δ_{er} and Δ_{er}, respectively, were -25.6 ± 1.9‰ and 17.8 ± 2.0‰ in 2001 and -26.6 ± 1.5‰ and 19.0 ± 1.6‰ in 2002. The results were in close agreement with $\delta^{13}C$ values derived from regional-scale atmospheric measurement programs for 2001, but less so in 2002, which had an unusual precipitation pattern. This suggests that regional-scale atmospheric sampling programs generally capture ecosystem $\delta^{13}C$ signals over Europe, but may be limited in capturing some of the interannual variations.

Correspondence: Dan Yakir, tel. + 972 (0)8 934 2549,
fax 972 (0)8 934 4124, e-mail: dan.yakir@weizmann.ac.il
[1]Present address: Hadley Centre for Climate Prediction and Research, Met Office, Fitzroy Road, Exeter EX1 3PB, UK.

© 2005 Blackwell Publishing Ltd

In 2001, but less so in 2002, there were discernable longitudinal and seasonal trends in δ_{er}. From west to east, across the network, there was a general enrichment in ^{13}C ($\sim$ 3‰ and $\sim$ 1‰ for the 2 years, respectively) consistent with increasing Gorczynski continentality index for warmer and drier conditions. In 2001 only, seasonal ^{13}C enrichment between July and September, followed by depletion in November (from about -26.0‰ to -24.5‰ to -30.0‰), was also observed. In 2001, July and August δ_{er} values across the network were significantly related to average daytime vapor pressure deficit (VPD), relative humidity (RH), and, to a lesser degree, air temperature (T_a), but not significantly with monthly average precipitation (P_m). In contrast, in 2002 (a much wetter peak season), δ_{er} was significantly related with T_a, but not significantly with VPD and RH. The important role of plant physiological processes on δ_{er} in 2001 was emphasized by a relatively rapid turnover (between 1 and 6 days) of assimilated carbon inferred from time-lag analyses of δ_{er} vs. meteorological parameters. However, this was not evident in 2002. These analyses also noted corresponding diurnal cycles of δ_{er} and meteorological parameters in 2001, indicating a rapid transmission of daytime meteorology, via physiological responses, to the δ_{er} signal during this season.

Organic matter $\delta^{13}C$ results showed progressive ^{13}C enrichment from leaves, through stems and roots to soil organic matter, which may be explained by ^{13}C fractionation during respiration. This enrichment was species dependent and was prominent in angiosperms but not in gymnosperms. $\delta^{13}C$ values of organic matter of any of the plant components did not well represent short-term δ_{er} values during the seasonal cycle, and could not be used to partition ecosystem respiration into autotrophic and heterotrophic components.

Keywords: carboeuroflux, CO_2 fluxes, ecosystem carbon budget, isotopic discrimination, ecosystem respiration, stable isotopes, $\delta^{13}C$

Received 19 December 2003; revised version received 9 September 2004; accepted 2 March 2005

Introduction

Global budgets of atmospheric CO_2 reflect an integration of net exchanges of CO_2 between terrestrial, oceanic and atmospheric reservoirs. In order to understand, model, and predict changes in instantaneous atmospheric CO_2 concentration, $[CO_2]$, it is necessary to understand the processes responsible for major fluctuations in CO_2 sources and sinks, and examine the relative contributions of these to global $[CO_2]$ changes. The main forest biomes (tropical, temperate and boreal forests) are the primary locations of terrestrial carbon storage, accounting for approximately 28% of global terrestrial surface area and about 80% and 41% of carbon stocks in vegetation and in soils, respectively (IPCC, 2001). The relative contributions of CO_2 sources and sinks in both the vegetation and soil of forest ecosystems change considerably over space and time, and many of the processes influencing these changes are not well understood.

The stable carbon isotopic composition, $\delta^{13}C$, of atmospheric CO_2 is a powerful tool for examining the relative contribution of specific CO_2 sources and sinks to total atmospheric $[CO_2]$ at local, regional and global scales (Tans *et al*., 1989, 1993; Lloyd & Farquhar, 1994; Ciais *et al*., 1995; Yakir & Wang, 1996; Fung *et al*., 1997; Bakwin *et al*., 1998; Battle *et al*., 2000; Buchmann & Kaplan, 2001). This is because processes associated with the exchange of CO_2 usually involve discrimination against the heavier carbon isotope, ^{13}C, relative to the lighter, ^{12}C (Farquhar *et al*., 1982; 1989; Ehleringer & Cerling, 1995), and these changes can be detected in isotopic measurements of atmospheric CO_2. Because isotopic mass balance is conserved within the earth–atmosphere–ocean system, a specific discrimination in a destination component will result in an equal and opposite discrimination in a source component. Hence, the global CO_2 budget may be expressed as an isotopic mass balance with respect to the time derivative of atmospheric $[CO_2]$ and $\delta^{13}C$:

$$\frac{d\delta_a}{dt} = \frac{1}{C_a}[F_{er}(\delta_{er} - \delta_a) - F_{ph}(\delta_{ph} - \delta_a) - F_{ao}(\delta_{ao} - \delta_a) + F_f(\delta_f - \delta_a) + F_{bb}(\delta_{bb} - \delta_a)], \quad (1)$$

where, symbols are defined in Table 1. The isotopic 'forcing' of any of the components in the land–ocean system (ecosystem respiration (er), photosynthesis (ph), etc.) on the atmosphere can be estimated from $\Delta = (\delta_{component} - \delta_a)$ with its effect on the atmosphere weighted by $F_{component}/C_a$. From this, it is clear that the isotopic Δ terms are critically important for estimating

Table 1 Symbols used (Gt is 10^{15} g)

Symbol	Description	Units
C_a	Average atmospheric CO_2 content	Gt C
c_a	CO_2 mole fraction in ambient atmosphere	μmol mol^{-1}
c_e	CO_2 mole fraction in ecosystem boundary layer	μmol mol^{-1}
c_{er}	CO_2 mole fraction of ecosystem respired CO_2 (excluding photorespiration)	μmol mol^{-1}
δ_a	$\delta^{13}C$ of ambient atmospheric CO_2	‰
δ_e	$\delta^{13}C$ of atmospheric CO_2 within the ecosystem boundary layer	‰
δ_{er}	$\delta^{13}C$ of ecosystem respired CO_2 (excluding photorespiration)	‰
δ_{ph}	$\delta^{13}C$ of net photosynthetic flux of CO_2 (excluding leaf dark respiration)	‰
δ_{oa}	$\delta^{13}C$ of ocean to atmosphere CO_2 transfer	‰
δ_{ao}	$\delta^{13}C$ of atmosphere to ocean CO_2 transfer	‰
δ_f	$\delta^{13}C$ of fossil fuel CO_2 flux	‰
δ_{bb}	$\delta^{13}C$ of biomass burning CO_2 flux	‰
F_{er}	Ecosystem CO_2 respiration flux (excluding photorespiration)	Gt C yr^{-1}
F_{ph}	Net photosynthetic flux of CO_2 (excluding leaf dark respiration)	Gt C yr^{-1}
F_{oa}	Ocean to atmosphere CO_2 transfer flux	Gt C yr^{-1}
F_{ao}	Atmosphere to ocean CO_2 transfer flux	Gt C yr^{-1}
F_f	Fossil fuel CO_2 flux	Gt C yr^{-1}
F_{bb}	Biomass burning CO_2 flux	Gt C yr^{-1}
Δ_{er}	^{13}C 'discrimination' associated with ecosystem respiration ($\delta_a - \delta_{er}$)	‰
Δ_{ph}	^{13}C 'discrimination' associated with plant photosynthesis ($\delta_a - \delta_{ph}$)	‰

the partitioning of land and ocean fluxes (Ciais *et al*., 1995). Δ values in the context of Eqn (1) are often termed 'discrimination' but are distinct from proper, chemical, isotopic discrimination between source and product, and normally refer to averages over a year for land/ocean partitioning studies (Tans *et al*., 1993; Ciais *et al*., 1995; Enting *et al*., 1995). Values for δ_a (where, $\delta = [(^{13}C/^{12}C_{sample})/(^{13}C/^{12}C_{standard}) - 1] \times 1000)$) and C_a are known accurately from measurements (e.g. Conway *et al*., 1994; Trolier *et al*., 1996), the ocean–atmosphere terms can also be estimated with reasonable confidence (Inoue & Sugimura, 1985; Broecker *et al*., 1986; Tans *et al*., 1993; Ciais *et al*., 1995), as can the fossil fuel (f) and biomass burning (bb) fluxes (Andres *et al*., 1996 1999; Randerson *et al*., 2002a; Levin *et al*., 2003; Marland *et al*., 2003; van der Werf *et al*., 2004). Often this means that land fluxes represent the major uncertainties.

A significant limitation in our understanding of land ecosystem functioning concerns the differentiation of CO_2 changes associated with respiration and photosynthesis, and their relative influence on net ecosystem CO_2 fluxes. To address this, Eqn (1) is also used to separate F_{er} and F_{ph} utilizing short time-scale (day to month) terrestrial ecosystem flux measurements. At these time- and spatial-scales the terms associated with oceanic and anthropogenic CO_2 fluxes can generally be ignored. Both Eqn (1) and any scaled-down version require good estimates of Δ_{er} ($\Delta_{er} = ''' \delta_{er} - \delta_a$) and Δ_{ph} ($\Delta_{ph} = \delta_{ph} - \delta_a$). This study includes estimates of Δ_{er}, which refer only to ecosystem respiration and is distinct from total ecosystem discrimination Δ_e which may be problematic if it involves both respiration and photosynthetic fluxes (cf. Buchmann *et al*., 1997).

Values of Δ_{er} should allow the comparison of the 'forcing' of ecosystem respiration on the atmosphere, accounting for variations in background δ_a, which can occur, for example, across large spatial distances or throughout seasonal cycles. Inverse models, that partition atmospheric CO_2 changes into their component oceanic and terrestrial sources and sinks, typically utilize estimated discrimination values, Δ, to parameterize the terrestrial ecosystem signal (Eqn (1)). However, as δ_a is not known, *a priori*, accurate determination of Δ requires reliable estimation of δ_a. In this study, we were particularly concerned with the sensitivity of Δ_{er} to estimates of δ_a, because, in principle, δ_a values could vary (by several per mils) between the $\delta^{13}C$ of night-time canopy air samples and the $\delta^{13}C$ of air above the planetary boundary layer (cf. Nakazawa *et al*., 1997; Hurwitz *et al*., 2004; Lai *et al*., 2004). Note that, in practical terms, δ_{er} and Δ_{er} (as well as the flux F_{er}) were obtained from night-time measurements which represent an integration of all ecosystem respiration components except photorespiration (which occurs in photosynthesising tissue during daylight). Likewise, F_{ph} and Δ_{ph} refer to the net photosynthetic flux and net photosynthetic ^{13}C discrimination, which include photorespiration.

The $\delta^{13}C$ values of ecosystem respired CO_2 are generally thought to be closely linked to that of CO_2 assimilated during recent photosynthesis owing to rapid cycling of photosynthate through the roots (e.g. Högberg *et al*., 2001; Bowling *et al*., 2002; Pataki *et al*., 2003). Integrated over time, Δ_{er} should, therefore, approach canopy photosynthetic discrimination, Δ_{ph}, and ideally, could be replaced by a single 'ecosystem discrimination' factor, Δ_e (e.g. Buchmann *et al*., 1997). However, the approach to equilibrium between Δ_{er} and Δ_{ph} is hindered by complex respiratory processes in the plant–soil system, and by continuous depletion of ^{13}C in atmospheric CO_2, from fossil fuel burning contributions, which result in a persistent disequilibrium (Quay *et al*., 1992; Tans *et al*., 1993; Fung *et al*., 1997). This disequilibrium is not well quantified, but has been estimated at $\Delta_{er}-\Delta_{ph} \approx 0.3‰$ (Fung *et al*., 1997). As noted, various definitions have been applied to the term 'discrimination' depending on the focus of the particular study and the conceptual approaches adopted (cf. Tans *et al*., 1993; Lloyd & Farquhar, 1994; Ciais *et al*., 1995; Trolier *et al*., 1996; Ehleringer *et al*., 1997; Fung *et al*., 1997; Bakwin *et al*., 1998; Bowling *et al*., 2001b; Buchmann & Kaplan, 2001; Miller *et al*., 2003; Scholze *et al*., 2003; Lai *et al*., 2004). In all cases, where Δ_{er} (or an equivalent term) is used in the context of Eqn (1) (i.e. as a 'forcing' term), it is conceptually distinct from the original biochemical definition of $\Delta = (^{13}C/^{12}C)_{source}/(^{13}C/^{12}C)_{product}-1$ (e.g. Farquhar *et al*., 1982) because, for example, atmospheric CO_2 is not the immediate source for respired CO_2.

While much effort has been invested in small-scale isotopic studies, only recently have ecosystem-scale applications become a major focus (cf. Buchmann & Kaplan, 2001 and references therein; Lai *et al*., 2004). Furthermore, relatively little data are available to develop isotopic perspectives at the regional or continental scale (Tans *et al*., 1996; Bakwin *et al*., 1998; Bousquet *et al*., 2000; Pataki *et al*., 2003; http://www.gcte-focus1.org/basin.html.). Recently, attempts have been also made to collect air samples from tall towers (Bakwin *et al*., 1995; Gloor *et al*., 2001) and aircraft (Nakazawa *et al*., 1993; Levin *et al*., 2002; Maksyutov *et al*., 2003), in order to obtain large scale isotopic data across planetary boundary layers.

In this study, we examine large-scale spatial and temporal trends in air samples derived δ_{er} and Δ_{er} values, and the $\delta^{13}C$ of leaf, stem and soil organic matter, and we compare these with corresponding flux tower ecophysiological and meteorological measurements. Finally, these data are used to provide ecosystem-based estimates of regional scale δ_{er} and Δ_{er}, and these are compared with estimates derived from air samples collected from background NOAA-CMDL stations. These provide a test to the hypothesis that $\delta^{13}C$ values derived from large-scale atmospheric measurements and models, which are routinely used to partition carbon fluxes between land and ocean, and potentially between respiration and photosynthesis on land, faithfully represent ecosystem-scale $\delta^{13}C$ values. In this framework, we also test the potential of $\delta^{13}C$ in canopy air and plant organic matter to record regional-scale ecophysiological patterns.

Methods

During 2001 and 2002, stable isotope measurements were made on air and organic matter samples collected from a network of forest sites participating in the Carboeuroflux project (continued from the original Euroflux project as described in Aubinet *et al*., 2000; Valentini, 2003). A total of 98 individual sampling campaigns were conducted between 2nd July 2001 and 26th November 2002, more during the growth periods. Samples were shipped to the stable isotope laboratory at the Weizmann Institute of Science in Rehovot, Israel, for analyses.

Here we outline the sampling and analytical methodologies used for the measurements of $[CO_2]$ and $\delta^{13}C$ of air sample CO_2, and $\delta^{13}C$ of plant and soil organic matter. We also detail the approaches used to estimate the $\delta^{13}C$ of ecosystem respired CO_2, δ_{er}, and ecosystem respiration 'discrimination', Δ_{er}. Specifics of the sites, methodology and results from all analyses are available at http://www.weizmann.ac.il/ESER/wp5/.

Network sites

The isotope network was composed of 13 sites in 2001 and extended to 16 in 2002 (Fig. 1, Table 2). Sites were selected mainly from existing carboeuroflux forest stations because these encompassed a wide range of climates (arctic, temperate, Mediterranean), species (including *Pinus*, *Quercus*, *Fagus*) and site characteristics (i.e. soil type, underlying bedrock, hydrology). These sites also provided detailed meteorological (flux tower) and ecophysiological data necessary to examine environmental/isotopic relationships. Most sites were located in continental Europe, although the full distribution ranged between Evora, Portugal in the west (8.0°W) to Yatir, Israel in the east (35.0°E), and Sodankylä, Finland in the north (67.4°N) to Yatir, Israel in the south (31.2°N).

Keeling plot approach and $\delta^{13}C$ of ecosystem respiration

The $\delta^{13}C$ of ecosystem respired CO_2, δ_{er}, was estimated using a 'Keeling plot' approach (Keeling, 1958, 1961;

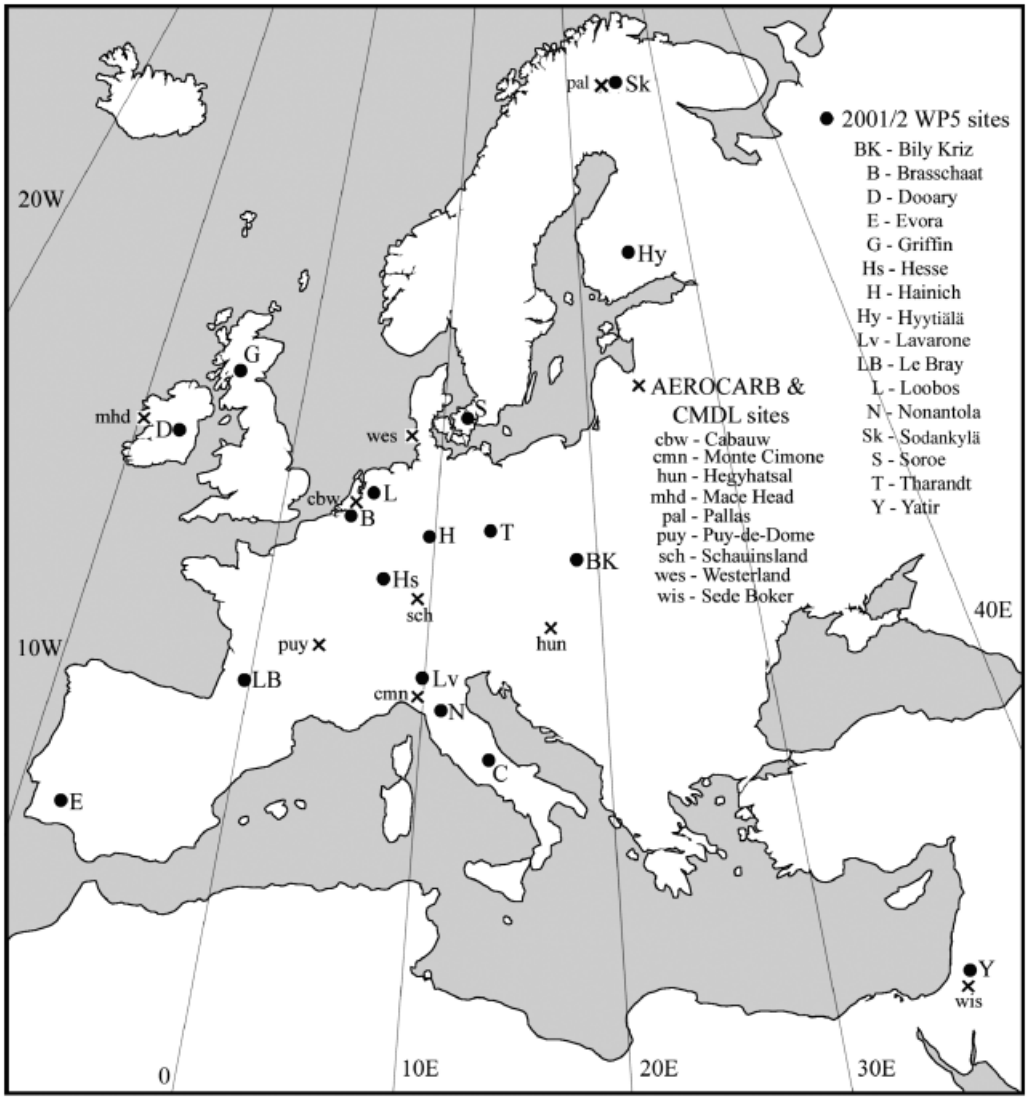

Fig. 1 Stable isotope network (WP5) sites for 2001 and 2002 (black circles). Also shown are the AEROCARB and NOAA/CMDL atmospheric [CO_2] monitoring sites for which data is used in this study (crosses).

Pataki *et al*., 2003). This utilizes a two end-member isotopic mass balance equation where CO_2 added (or removed) by a net source (or sink) is mixed into a constant background atmospheric CO_2. It is assumed that the [CO_2] and $\delta^{13}C$ of these two end-members are constant during the period of sampling, such that air samples collected within the ecosystem boundary layer, which have varying [CO_2] and $\delta^{13}C$ values, should differ only in their relative proportions of ecosystem respired CO_2 and initial atmospheric CO_2. Therefore, a plot of $1/[CO_2]$ vs. $\delta^{13}C$, the conventional Keeling plot, should show the ecosystem air samples distributed along a straight line delimited by background atmospheric CO_2 at one extreme, and pure ecosystem respired CO_2 at the other.

For this study, all air samples were collected from within the ecosystem boundary layer at night-time , and it was assumed that the [CO_2] and $\delta^{13}C$ of the sampled air, c_e and δ_e, well represented the sum of the background atmospheric [CO_2] and $\delta^{13}C$, c_a and δ_a, and the [CO_2] and $\delta^{13}C$ of ecosystem respired CO_2, c_{er} and δ_{er}:

$$c_e\delta_e = c_a\delta_a + c_{er}\delta_{er}. \quad (2)$$

In practice, the assumptions and application of the Keeling plot approach need to be considered carefully because δ_e values are usually far removed from the δ_{er} values that are estimated. Consequently, errors or bias in the air sample values can be attenuated significantly in δ_{er} estimates (see Pataki *et al*., 2003 for a detailed

Table 2 Background information on the 17 sites participating in the 2001/2 stable isotope network

Site, Country	Lat (°N)	Lon (°E)	Elev (masl)	Dominant Species	P_{ann} (mm)	T_{ann} (°C)	Investigators
Bily Kriz, Czech Republic	49.5	18.5	898	*Picea abies*	1100	4.9	Dalibor Janous , Zuzana Rosova, Katarina Havrankova
Brasschaat, Belgium	51.3	4.5	16	*Pinus sylvestris/ Quercus robur*	750	10.0	Arnaud Carrera, Ivan Janssens
Collelongo, Italy	42.4	11.9	1150	*Fagus sylvatica*	1180	6.3	Giorgio Matteucci, Catarina Mata, Andrea Scartazza
Dooary, Ireland	52.3	−7.9	260	*Picea sitchensis*	804	9.3	Kevin Black, Bruce Osborne
Evora, Portugal	38.5	−8.0	235	*Quercus ilex/ Quercus suber*	920	14.2	João Santos Pereira, Cathy Besson
Griffin, Scotland	56.6	−3.8	340	*Picea sitchensis*	1200	8.0	John Moncrieff, Paul Jarvis, Robert Clement
Hainich, Germany	51.1	10.5	445	*Fagus sylvatica*	750	7.0	Nina Buchmann, Alexander Knohl
Hesse, France	48.6	7.1	300	*Fagus sylvatica*	885	9.2	Andre Granier, Patrick Gross, Marianne Peiffer
Hyytiälä, Finland	61.5	24.2	170	*Pinus sylvestris*	640	3.5	Timo Vesala, Petri Keronen, Mari Pihlatie
Lavarone, Italy	45.9	11.3	150	*Abies alba*	1150	6.9	Alessandro Cescatti, Barbara Marcolla
Le Bray, France	44.7	−0.8	60	*Pinus pinaster*	950	13.5	Paul Berbiger, Andrew Kowalski, Regis Burlett
Loobos, Netherlands	52.1	5.6	25	*Pinus sylvestris*	786	9.8	Eddy Moors, Jan Elbers
Nonantola, Italy	44.6	11.1	25	*Quercus robur/ Fraxinus spp.*	1000	14.5	Francesca Ponti, Federica Rossi, Osvaldo Facini
Sodankylä, Finland	67.4	26.7	180	*Pinus sylvestris*	500	−1.0	Tuomas Laurila, Mika Aurela
Soroe, Denmark	55.0	11.6	42	*Fagus sylvatica*	510	8.1	Per Ambus, Kim Pilegaard
Tharandt, Germany	50.9	13.5	380	*Picea abies*	820	7.7*	Christian Bernhofer, Barbara Köstner, Thomas Grünwald
Yatir, Israel	31.2	35.0	680	*Pinus halepensis*	275	22.0	Dan Yakir, Debbie Hemming

*1959–2000 mean.

Included are site latitude, Lat, longitude, Lon, elevation in meters above sea level, Elev (masl), dominant tree species, Dominant Species, annual precipitation sum, P_{ann}, mean annual air temperature, T_{ann}, and the main investigators involved, Investigators.

discussion). We try to minimize errors and bias by, (1) developing a sampling strategy that balances the practical requirements of air sampling in forest ecosystems with the assumptions underlying Eqn (2), and (2) adopting a rigorous procedure for the removal of outliers and errors in the regression analyses. These are discussed further below.

To estimate δ_{er} from ecosystem air samples, we rearranged Eqn (2), substituting in the equation for conservation of mass, $c_e = c_a + c_{er}$, to give the following equation:

$$c_e\delta_e = \delta_{er}c_e + c_a(\delta_a - \delta_{er}), \quad (3)$$

where, δ_{er} is the slope of a regression line relating $c_e\delta_e$ to c_e. Note that Eqn (3) is simply a rearrangement of the conventional Keeling plot equation and is termed here the 'slope method' (cf. Miller *et al*., 2003).

The Model II geometric mean regression (GMR) technique (Sokal & Rholf, 1995) was used to fit regression lines to the slope method data. This was preferred over the conventional least-squares regression technique because it accounts for uncertainty in both the *x*- and *y*-axis values, thus ensuring that the slope and intercept values are not subject to a systematic bias (Miller & Tans, 2003; Pataki *et al*., 2003). It was noted, however, that δ_{er} values derived using the slope method and conventional Keeling plot methods are not identical, potentially hindering comparisons between data obtained by the two methods. Figure 2 shows that where the SE of the δ_{er} estimate was below 4.0‰, the differences between methods were below 0.84‰, decreasing to <0.35‰ for SEs less than 2.0‰, and <0.2‰ for SEs less than 1.0‰. Using low SE data minimized this potential problem.

Treatment of errors and outliers

As practical constraints on sampling limited the number of air samples collected during each campaign to approximately 10, the linear regression fit, and therefore, the estimated δ_{er} values, could be rather sensitive to inaccuracies in individual data points.

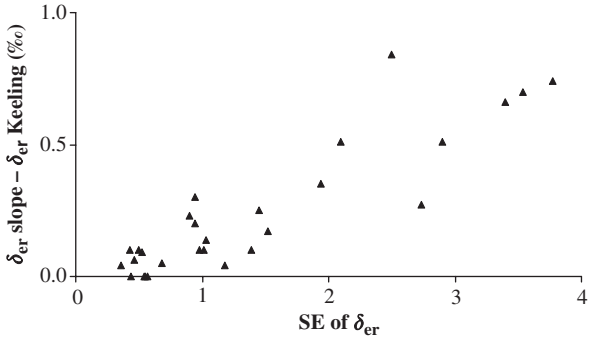

Fig. 2 Differences in $\delta^{13}C$ of ecosystem respired CO_2, δ_{er}, estimates using a geometrical mean regression of either the slope (δ_{er} slope) or conventional Keeling plot intercept (δ_{er} Keeling) methods as a function of the SE of the δ_{er} estimate.

Although some errors could be reduced through sampling strategy , a further two-step filtering procedure was adopted for the identification and removal of outliers from each set of air sample results. In this procedure, data points greater than two standard deviations (SDs) away from the regression line were ignored, and the error of each δ_{er} estimate was approximated as the SE of the slope of the least squares linear regression (Miller & Tans, 2003). If the SE was less than 2.0‰, these estimates were included in further analyses. For δ_{er} estimates with SEs above 2.0‰, data points greater than 1 SD away from the regression line were also ignored, and the δ_{er} and SE values were recalculated. Six data points were regarded as the minimum number necessary for a δ_{er} estimate, therefore, δ_{er} estimates with SEs less than 2.0‰ and six or more data points were accepted for further analyses. A SE of 2.0‰ was chosen because it showed relatively low differences between the slope and Keeling plot δ_{er} estimations (noted above), and it also provided a reasonable balance between accuracy and sample number; a SE threshold of 1.0‰ would have excluded over 60% of the δ_{er} estimates, reducing the spatial and temporal coverage significantly. Using these selection criteria $\sim 30\%$ of the δ_{er} estimates were eliminated (Table 3), and $\sim 10\%$ of points that compose all of the selected slope method regression lines were ignored.

Estimation of Ecosystem Respiration Discrimination

For the application of Δ_{er} as defined in the Introduction, we were concerned with its sensitivity to estimates of δ_a. Strictly, from the derivation in Eqns (2) and (3), δ_a is the $\delta^{13}C$ value of atmospheric CO_2 into which respired CO_2 with δ_{er} value is mixed; and therefore δ_a and c_a will necessarily define some point along the Keeling plot mixing line. This point will be between the $\delta^{13}C$ of night-time canopy air samples and the $\delta^{13}C$ of air above the planetary boundary layer, which may involve a range of a few per mil. However, in reality δ_a can be determined in various ways, which will have consequences for the estimation of Δ_{er}. Therefore, we compared three methods for estimating δ_a, detailed below, using the 2001 data. Methods 1 and 2 determine δ_a utilizing the equations of the slope method regression lines, and Method 3 uses an independent δ_a record from a single central European site to represent all sites.

For Method 1, we take advantage of the fact that while there are only two stations recording δ_a across Europe, there are nine well-distributed stations recording c_a (NOAA/CMDL, CSIRO or AEROCARB, see Fig. 1). For each of our network sites and sampling dates, we adopted c_a values that were recorded at the nearest of the nine measurement stations during the period closest to the date when isotope samples were collected. Using these adopted c_a values and the corresponding site/sampling date regression line relationship (derived from the slope method fit), estimates of δ_a were derived.

In practice, the relationship between δ_e and c_e previously established (Eqn (3)): $c_e\delta_e = mc_e + n$, was evaluated at values of c_e equal to c_a, the background atmosphere. As c_e and δ_e represent a point on a mixing line between c_a, δ_a of the background atmosphere at one extreme and c_{er}, δ_{er} of respired CO_2 at the other, as we move along this line away from the respired CO_2 source, the influence of respired CO_2 on c_e and δ_e will diminish, tending toward c_a, δ_a.

Values for δ_{er} and $c_a(\delta_a - \delta_{er})$ were obtained from the slope and intercept of each specific mixing model regression line, and the c_a ($= c_e$) values from trend lines fitted through the c_a time series of nine NOAA/CMDL, CSIRO or AEROCARB background air sampling stations located within reasonably close proximity to our network sites (Fig. 1). Records of c_a from stations closest to each network site were used. Usually, the distance between the network site and the c_a measurement station was less than 500 km, although for the Finland, Hyytiälä and Portugal, Evora sites the δ_a estimates were from c_a station data ~ 1000 km away.

For Method 2, it is assumed that short-term (up to 2 weeks) changes in the c_a and δ_a at a specific site were negligible. This meant that the c_a and δ_a of one sampling campaign was nearly equal to the c_a and δ_a of a consecutive campaign from the same site within the 2-week time window. The slope method regression equations from these two campaigns could, therefore, be equated assuming that they intersect each other at c_a

Table 3 Data from air flask sampling campaigns during 2001 and 2002

Site	Date	δ_{er} (‰)	SE (‰)	$\langle[CO_2]\rangle$ (ppm)	n	T_a (°C)	P_m (mm)	RH (%)	VPD (kPa)
Brasschaat, Belgium	02/07/01	−26.4	0.6	191.3	10	19.7	51.8*	77.3	0.52
Brasschaat, Belgium	03/07/01	−26.4	0.5	98.5	10	22.7	51.8*	61.9	1.05
Griffin, Scotland	03/07/01	−27.1	0.6	100.9	10	17.1	43.3*	80.4	0.38
Griffin, Scotland	09/07/01	−25.6	0.9	106.7	9	12.1	43.3*	69.6	0.43
Nonantola, Italy	10/07/01	−23.9	0.9	133.1	13	24.7	98.8	70.9	0.91
Hesse, France	25/07/01	−25.9	0.5	79.9	11	23.7	99.2	61.0	1.14
Hainich, Germany	02/08/01	−24.6	0.5	73.7	7	19.2	106.9†	62.3	0.84
Griffin, Scotland	13/08/01	−27.6	0.4	167.1	10	17.4	40.5	86.9	0.26
Tharandt, Germany	14/08/01	−23.5	1.5	27.8	7	23.6	51.9	61.0	1.13
Brasschaat, Belgium	28/08/01	−24.1	0.5	64.9	10	17.5	59.9	64.8	0.70
Brasschaat, Belgium	29/08/01	−26.2	0.9	60.8	7	17.5	59.9	67.7	0.64
Griffin, Scotland	10/09/01	−24.0	1.0	52.5	10	10.1	96.4	71.0	0.36
Nonantola, Italy	20/09/01	−24.7	0.4	101.5	14	16.6	151.6	65.2	0.66
Hainich, Germany	25/09/01	−26.4	1.0	27.9	7	11.2	142.4	77.3	0.30
Loobos, Netherlands	25/09/01	−23.6	0.4	153.3	7	13.8	176.7	83.1	0.27
Tharandt, Germany	07/10/01	−25.0	1.9	39.7	10	16.5	42.6	72.7	0.51
Loobos, Netherlands	16/10/01	−27.1	0.7	114.1	7	15.0	72.6	67.1	0.56
Hainich, Germany	18/10/01	−29.0	1.2	15.7	7	8.9	21.7	96.7	0.04
Brasschaat, Belgium	01/11/01	−30.0	1.4	78.3	10	10.6	70.7‡	79.9	0.26
Bily Kriz, Czech Republic	13/11/01	−22.1	1.4	15.9	9	−1.8	136.3	82.6	0.09
Yatir, Israel	20/11/01	−27.1	1.0	5.8	16	15.2	4.0	75.4	0.43
Collelongo, Italy	26/11/01	−23.5	1.5	9.2	11	−0.4	n/a	79.7	0.12
Evora, Portugal	04/12/01	−26.3	0.3	40.9	11	9.9	n/a	88.1	0.15
Tharandt, Germany	04/04/02	−27.3	1.3	28.6	9	7.3	38.5	40.2	0.61
Evora, Portugal	19/04/02	−31.0	1.3	4.3	17	17.2	n/a	79.4	0.40
LooBos, Netherlands	23/04/02	−26.5	0.8	80.3	8	14.6	20.0	68.0	0.53
Soroe, Denmark	23/04/02	−28.7	1.1	35.7	9	11.4	40.8	75.1	0.34
Dooary, Ireland	24/04/02	−25.0	0.9	38.1	10	9.4	79.0	84.9	0.18
Bily Kriz, Czech Rep.	07/05/02	−24.6	1.1	20.9	6	16.4	132.4	79.7	0.38
LooBos, Netherlands	09/05/02	−26.7	1.1	63.5	8	18.8	148.4	70.5	0.64
Hainich, Germany	15/05/02	−27.7	1.9	66.3	9	13.0	112.1	65.6	0.51
Yatir, Israel	15/05/02	−28.6	2.0	7.6	15	17.1	0.0	72.0	0.55
Nonantola, Italy	20/05/02	−26.5	0.4	100.9	12	19.7	183.2	74.4	0.59
Tharandt, Germany	03/06/02	−26.9	1.6	56.4	9	17.4	67.8	52.7	0.94
Hesse, France	14/06/02	−27.7	1.2	60.1	10	22.4	68.0	n/a	n/a
Nonantola, Italy	17/06/02	−26.3	0.6	105.8	9	30.0	90.0	65.6	1.46
Hyytiälä, Finland	11/07/02	−29.0	1.0	29.0	6	22.9	71.3	60.8	1.10
Dooary, Ireland	12/07/02	−27.1	1.1	77.2	9	15.4	34.9	69.2	0.54
Hainich, Germany	20/07/02	−27.9	0.9	43.8	10	17.5	84.0	64.0	0.72
Nonantola, Italy	22/07/02	−26.2	0.9	50.7	7	28.3	212.8	67.2	1.26
Lavarone, Italy	23/07/02	−26.5	0.7	57.1	9	17.0	n/a	79.2	0.40
Collelongo, Italy	24/07/02	−26.7	1.5	25.2	10	n/a	n/a	n/a	n/a
Brasschaat, Belgium	28/07/02	−25.6	0.4	49.8	8	24.8	68.8	63.4	1.14
LooBos, Netherlands	29/07/02	−26.3	0.4	124.7	16	27.1	90.2	49.3	1.82
Tharandt, Germany	30/07/02	−26.4	0.6	103.6	9	26.1	68.4	42.8	1.94
Sodankyla, Finland	01/08/02	−27.6	0.8	53.3	10	13.4	144.5†	66.6	0.51
LooBos, Netherlands	15/08/02	−26.9	0.3	90.1	9	23.8	28.8	60.2	1.17
Hainich, Germany	16/08/02	−25.9	0.7	56.4	6	21.1	101.9	61.0	0.98
Soroe, Denmark	16/08/02	−26.8	1.0	160.1	10	24.3	97.9	78.9	0.64
Brasschaat, Belgium	19/08/02	−27.1	0.6	52.8	10	22.0	243.7	82.8	0.45
Nonantola, Italy	27/08/02	−26.1	0.4	92.9	10	23.2	109.2	77.9	0.63
Brasschaat, Belgium	29/08/02	−27.3	0.4	90.3	10	18.8	243.7	80.0	0.43
Bily Kriz, Czech Rep.	29/08/02	−25.6	0.7	36.5	10	31.0	216.4	79.0	0.94

(continued)

Table 3 (Contd.)

Site	Date	δ_{er} (‰)	SE (‰)	$\langle[CO_2]\rangle$ (ppm)	n	T_a (°C)	P_m (mm)	RH (%)	VPD (kPa)
Dooary, Ireland	04/09/02	−25.4	0.9	37.7	13	13.1	23.5	92.0	0.12
Hyytiälä, Finland	12/09/02	−26.9	0.2	113.1	12	15.6	13.5	75.8	0.43
Hainich, Germany	16/09/02	−24.2	1.9	27.5	10	11.4	38.3	69.3	0.41
LooBos, Netherlands	18/09/02	−27.4	0.5	75.9	10	14.6	76.0	79.5	0.34
Lavarone, Italy	18/09/02	−25.8	0.6	52.3	10	12.5	n/a	72.8	0.40
Tharandt, Germany	19/09/02	−26.7	0.7	61.7	9	13.9	53.3	65.1	0.56
Nonantola, Italy	30/09/02	−25.5	0.6	97.0	8	14.3	136.8	68.6	0.51
Soroe, Denmark	09/10/02	−29.7	1.0	14.3	9	6.5	154.2	75.6	0.24
Lavarone, Italy	16/10/02	−24.9	0.5	58.1	10	10.7	n/a	78.8	0.27
Tharandt, Germany	29/10/02	−26.7	0.3	100.7	10	6.1	92.3	72.8	0.26
LooBos, Netherlands	31/10/02	−27.0	0.8	47.3	10	8.4	67.8	75.0	0.28
Nonantola, Italy	07/11/02	−25.0	0.8	73.4	6	5.5	100.0	86.9	0.12
Collelongo, Italy	20/11/02	−27.5	1.2	26.2	10	n/a	n/a	n/a	n/a
δ_{er} estimates below have SEs >2.0 and are not used in analyses									
Hainich, Germany	24/07/01	−29.4	2.5	70.3	10				
Tharandt, Germany	12/08/01	−24.2	2.9	21.5	6				
Yatir, Israel	20/09/01	−14.1	4.3	27.0	20				
Hyytiälä, Finland	09/10/01	−23.0	8.1	4.3	10				
Tharandt, Germany	11/10/01	−26.1	3.4	12.9	8				
Collelongo, Italy	18/10/01	−34.7	4.0	14.1	19				
Nonantola, Italy	30/10/01	−35.1	3.5	13.8	12				
Le Bray, France	31/10/01	−30.4	3.8	25.2	10				
Brasschaat, Belgium	05/11/01	−24.5	2.1	61.3	9				
Bily Kriz, Czech Republic	06/11/01	−31.9	2.7	10.1	9				
Le Bray, France	07/11/01	−50.1	29.8	2.1	10				
Yatir, Israel	15/04/02	−23.7	2.0	22.7	20				
Collelongo, Italy	29/04/02	−30.5	2.2	13.6	20				
Brasschaat, Belgium	08/05/02	−28.1	2.0	28.0	20				
Bily Kriz, Czech Rep.	15/05/02	−25.6	2.7	27.4	10				
Soroe, Denmark	04/06/02	−31.8	2.1	10.1	10				
Collelongo, Italy	11/06/02	−23.5	4.1	30.4	20				
Hainich, Germany	13/06/02	−32.5	1.0	50.0	9				
Bily Kriz, Czech Rep.	19/06/02	−26.6	2.1	29.5	10				
Evora, Portugal	28/06/02	−23.6	3.7	4.4	10				
LooBos, Netherlands	16/07/02	−27.7	0.4	20.2	10				
Le Bray, France	19/07/02	−25.3	2.1	38.0	10				
Hesse, France	22/07/02	−30.5	1.1	39.2	9				
Collelongo, Italy	21/08/02	−27.6	2.3	28.2	8				
Evora, Portugal	25/09/02	−31.6	3.5	11.6	10				
Collelongo, Italy	27/09/02	−27.8	1.9	13.5	12				
Brasschaat, Belgium	09/10/02	−31.2	2.4	8.8	10				
Brasschaat, Belgium	13/10/02	−27.8	2.0	8.0	10				
Hainich, Germany	19/10/02	−20.0	2.2	27.2	7				
Evora, Portugal	26/11/02	−31.8	5.4	8.0	10				

*June average; †July average; ‡October average.

Listed are estimates of the $\delta^{13}C$ of ecosystem respired CO_2, δ_{er}, the standard error of the δ_{er} estimate, SE, the $[CO_2]$ range over which samples were collected, $\langle[CO_2]\rangle$, the number of samples used to derive δ_{er}, n, and daytime average temperature, T_a, relative humidity, RH, vapor pressure deficit, VPD, and monthly precipitation sum, P_m. Estimates of δ_{er} with a SE > 2.0‰ are listed at the bottom of the table, these are not used in further analyses. n/a means data not available.

and δ_a:

$$c_a = \frac{n_2 - n_1}{(\delta_{er1} - \delta_{er2})}, \quad (4)$$

$$\delta_a = \frac{\delta_{er} c_a + n}{c_a}. \quad (5)$$

In these equations, the subscripts 1 and 2 refer to two consecutive sampling campaigns, and n is the mixing model equation intercept on the y-axis $c_a(\delta_a - \delta_{er})$. Note that in Eqn (5), δ_{er} and n values from either sampling campaign could be utilized. This method did not provide estimates of δ_a throughout the sampling season because campaigns were not always made within a 2-week time interval. However, these values provide a useful comparison with δ_a values estimated from the other methods.

For Method 3, the measured δ_a values (NOAA/CMDL) from Hegyhatsal, Hungary were assumed to be representative of the variations in δ_a of the entire network. The specific δ_a values for each sampling campaign were estimated from the equation of 5th-order polynomial trend lines fitted through the annual data (to avoid bias in the polynomial trends from exaggeration of end points, lines were fitted to 16 months of δ_a data, 2 extra months before and after each year; Fig. 3).

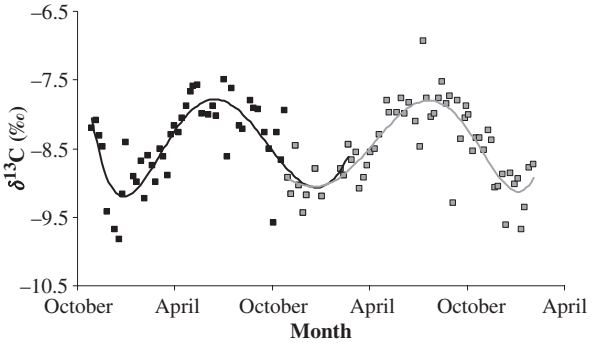

Fig. 3 Carbon isotopic composition ($\delta^{13}C$) of atmospheric CO_2 measured on NOAA-CMDL flask samples collected at Hegytatsal, Hungary during 2001 (filled) and 2002 (squares). Tick marks on the x-axis are on the 1st day of the month. Trend lines for each year are fitted with 5th order polynomial equations covering a 16-month period, 2 extra months before and after each year, to avoid bias on the end points.

Air and organic matter sampling

Sampling strategy

The air sampling strategy adopted was a balance between satisfying the assumptions of the Keeling plot approach, while allowing enough flexibility to accommodate the considerable diversity of ecosystems, environmental conditions and $[CO_2]$ and $\delta^{13}C$ ranges that exist between the network sites.

One of the key assumptions of the Keeling plot (or slope method) is that there are only two end members. Sampling was conducted at night-time, 2 h after dark and before dawn, in an attempt to isolate the isotopic signal of δ_{er} from the combined signals of photosynthesis and respiration that occur during the day. Sampling at night also avoided significant thermally driven convection and advection, which encourage the transport of CO_2 in unrepresentative plumes or from long-range sources outside the typical forest footprint. Nevertheless, it must be noted that nonforest sources of CO_2, such as from fossil fuel burning or other nearby ecosystems, may significantly influence the night-time air samples, particularly during periods of high horizontal advection or in polluted regions when ecosystem activity is low (Florkowski *et al.*, 1998; Potosnak *et al.*, 1999; Takahashi *et al.*, 2001; Demény & Haszpra, 2002; Still *et al.*, 2003).

To determine the specific heights and times for each air sampling, the pattern of nocturnal $[CO_2]$ changes, measured in air from the top of each flux tower (a few meters above the forest canopy), were examined for 1–2 weeks prior to sampling. The typical time span of maximum $[CO_2]$ ranges was used to delimit the timing of flask sampling. Ideally, air samples were collected across this interval from the tower top height in order to maximize the footprint area, and allow mixing of different ecosystem CO_2 sources (soil, stem, leaf). However, in practice, at many sites and times this $[CO_2]$ range was less than 20 ppm, and it was known that the standard error (SE) of δ_{er} estimates could increase significantly with $[CO_2]$ ranges below 50 ppm (Pataki *et al.*, 2003). To minimize such errors, the initial strategy was to include air samples from progressively lower heights until a 50 ppm range was obtained. After the 2001 results were analyzed, this range was reduced to 30 ppm, because it proved to be a threshold below which the SE of the δ_{er} estimate tended to increase rapidly above 2.0‰ (Fig. 4).

Despite these sampling considerations, it often proved difficult to obtain a nocturnal $[CO_2]$ range of 30 ppm, especially at the drier sites (i.e. Evora, Portugal and Yatir, Israel) and in many cases this range was only reached by sampling air from within or below the canopy. This highlights another possible source of bias in our δ_{er} signals because of over-representation of the soil respired CO_2 flux (Pataki *et al.*, 2003). Using this approach, it should also be remembered that a net ecosystem δ_{er} signal can contain, sometimes significant, contributions from understorey vegetation (Swanson &

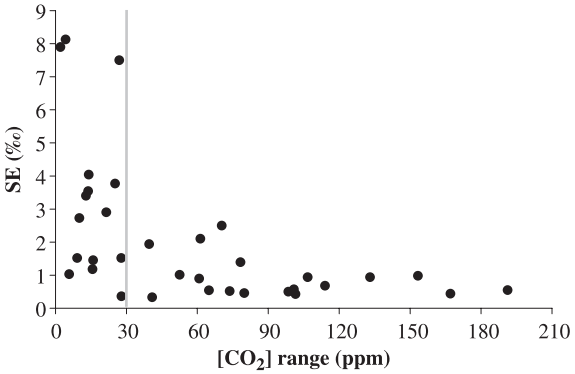

Fig. 4 Standard error (SE) of the 2001 δ_{er} estimates vs. the $[CO_2]$ range over which air samples were collected. Below 30 ppm (vertical grey line) the average SE increases rapidly, hence this was used as a threshold $[CO_2]$ range to aim for during sample collection.

Flanagan, 2001). Although, these are unavoidable features of such δ_{er} estimations, for most ecosystems they are not believed to be significant enough to invalidate the δ_{er} signal.

Equipment and collection

Boxes containing 20 200 mL glass flasks, a chemical drying unit (magnesium per-chlorate hydrate), connection accessories and at least six Exetainers (LABCO; Buckinghamshire, UK Exetainer #739W/GL, 12 mL) were cycled (via airmail) between each network participant and the central isotope laboratory at the Weizmann Institute. Flasks were preflushed with dry air of low $[CO_2]$ to provide an analytical indicator of incomplete sampling.

A novel, low cost, flask sampling kit was used to collect ecosystem air samples. It consisted of a special two-layer inlet tube-attachment, a drying unit (packed with magnesium perchlorate and indicating drierite), a single-stopcock (Glass Expansion, West Melbourne, Australia) 200 mL glass flask and an air pump. The two-layer tubing attachment allowed airflow through the single-stopcock valve into the flask through the small, inner tube and out via the wider, external surround. The system was designed to be integrated in-line with existing flux tower air sampling equipment; between the outlet of the infrared gas analyser (IRGA) and the inlet of the air pump. This enabled constant monitoring of $[CO_2]$ during sample collection, and minimal interference with normal flux tower operations. Using an external air pump and IRGA, the system was also used independently to collect air samples from other locations. During sampling each flask was flushed with at least 2 L of dried air to ensure complete turnover of the flask volume (as previously tested).

Samples of leaves, stem and soil from the dominant species at each site were collected on the day of, or the day after, air sampling. Leaf samples (~ 1.5 g fresh weight) of the dominant species were taken from fully expanded cohorts growing in sunny and ventilated locations. When possible, samples were collected at the time of maximum photosynthesis (a consideration for leaf–water analyses), and for broadleaf species, the petiole and major vein were removed. Small (<5.0 mm diameter), nongreen, stem samples were taken from the same location as the leaf sampling, and soil was collected from the surface 0.0–5.0 cm at locations representative of the site. Immediately after sampling, the organics were transferred into vacuum tight Exetainers such that $\sim 75\%$ of the Exetainer was filled.

Shipping time from the sampling sites to the Weizmann laboratory was usually less than 2 weeks, and air sample analyses were completed within a few days of arrival. No effect of storage on the isotopic or CO_2 concentration results was detected even after 2 months (data not shown). It is possible that some degree of decomposition occurred during transportation of the organic matter samples. As no clear visible signs of this were evident, its influence on the isotopic composition of bulk organic carbon is believed to be small. On arrival, organic matter samples were stored at $-15.0\,^{\circ}C$ prior to analysis.

Analyses

Air samples

The $\delta^{13}C$ of CO_2 in air was analyzed using a continuous flow mass spectrometer configuration with a 15 flask automatic manifold system. An aliquot of 1.5 mL of air was expanded from each flask into a sampling loop on a 15-position valve (Valco Houston, TX, USA). CO_2 was cryogenically trapped from the air samples using Helium as a carrier gas, it was then separated from N_2O with a Carbosieve G packed column at $70\,^{\circ}C$, and analyzed on a Europa 20-20 Isotope Ratio Mass Spectrometer (Crewe, UK). $\delta^{13}C$ results are quoted in parts per thousand (‰) relative to the VPDB international standard (Coplen, 1994). The analytical precision was ± 0.1‰.

To measure $[CO_2]$, an additional 40.0 mL sub-sample of air from each flask was expanded into a mechanical bellows and then passed through an infra-red gas analyzer (LICOR 6262; Lincoln, NE, USA) in an automated system similar to that of Bowling *et al.* (2001a). The precision of these measurements was 0.1 ppm.

The [CO_2] and $\delta^{13}C$ of dry cylinder air obtained in Israel was calibrated locally and for each cylinder, samples were tested by sample intercomparison with NOAA-CMDL (Boulder, CO, USA) (cf. Trolier *et al.*, 1996), with precisions of 0.1 ppm and 0.01‰. This air was used to calibrate dry air from other cylinders in the Weizmann laboratory, which were adopted as working standards. Flasks filled with calibrated standard air were measured with each batch of 10 sample flasks; five standards were measured per 10 samples for $\delta^{13}C$ analyses, and four standards per 10 samples for [CO_2] analyses.

Organic matter samples

Leaf, twig and soil samples were dried by vacuum distillation at 60 °C, bark was removed from the stems. Leaf and twig samples were then milled using a Wiley Mill fitted with size 40 mesh, and soil samples were ground in a pestle and mortar. Soils containing carbonates were treated with 1 M hydrochloric acid. Between 0.2 and 0.4 mg of each dry sample were weighed into tin capsules (Elemental Microanalysis Ltd., Okehampton, UK, $3\,mm^2 \times 5\,mm^2$ #D1002), and their $\delta^{13}C$ was determined using an elemental analyzer linked to a Micromass (Manchester, UK) Optima IRMS.

Three replicates of each sample were analyzed and two samples of a laboratory working standard cellulose ('WC') were measured for every 12 samples. Four samples of the Acetanilide (Elemental Microanalysis Ltd., #B20CC) international standard were used to calibrate each run, and a correction was applied to account for the influence of a blank cup. The precision was $\pm$ 0.1‰.

Results

Spatial and temporal variations in δ_{er} and prevailing meteorology

Estimates of δ_{er} were made for 34 individual air sampling nights in 2001 and 65 in 2002 (Table 3). Around 70% of these (23 in 2001 and 46 in 2002) passed the selection criteria (see Methods) and were utilized in the analyses. The average and SD of δ_{er} in 2001 and 2002 were -25.6 ± 1.9‰ and -26.6 ± 1.5‰, respectively. This change was not attributed to the difference in sampling sites and times between 2001 and 2002, as similar average δ_{er} values were obtained for the 2002 season with either a whole season (and site) average or an average composed of only data from the same sites and sampling period (July–November) as the 2001 samples.

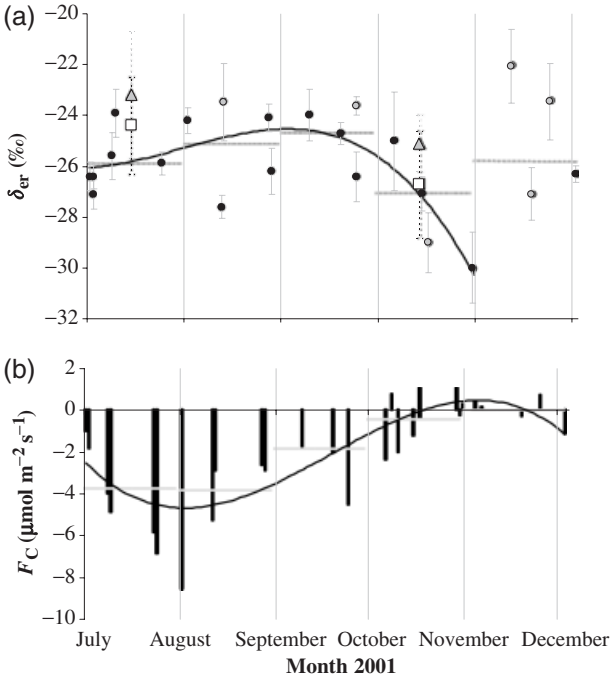

Fig. 5 2001 seasonal variations in (a) $\delta^{13}C$ of ecosystem respired CO_2, δ_{er}, (circles) and (b) 24 h averaged (00:00–23:30 hours on the air sampling day) net ecosystem exchange, F_c (bars). Grey circles highlight δ_{er} values estimated with [CO_2] ranges <30 ppm (not used in data analysis; see Method for details). Error bars delimit the standard error of the δ_{er} estimate. Horizontal stippled lines are monthly average values and thick black lines represent 3rd-order polynomial fits. Large symbols (dashed lines for SE) show the δ_{er} values estimated from air sampled at two NOAA/CMDL network stations, Mace Head, Ireland (grey triangles) and Hegyhatsal, Hungary (open squares), between June–August and September–November. Gridlines highlight the 1st day of each month. Note that November and December are omitted from the smoothed line fit because these values are generally for sites where seasonal photosynthetic activity is largest during winter, as such their seasonal trends could be expected to be different from results from the other sites.

Despite considerable scatter, a seasonal trend was discernable in the individual and monthly average δ_{er} values for 2001. This showed enrichment in ^{13}C from around -26.0‰ to -24.5‰ between July and September, followed by depletion to -30.0‰ in November (Fig. 5a, Table 3). In contrast, no clear seasonal trends were evident in the 2002 results, although average September δ_{er} was a little higher (at least 0.6‰) than in other months (Fig. 6a, Table 3), and the variance in δ_{er} across the network was lower between July and September, suggesting a stronger common signal during this period. Between years, the largest differences in the monthly average δ_{er} values were observed

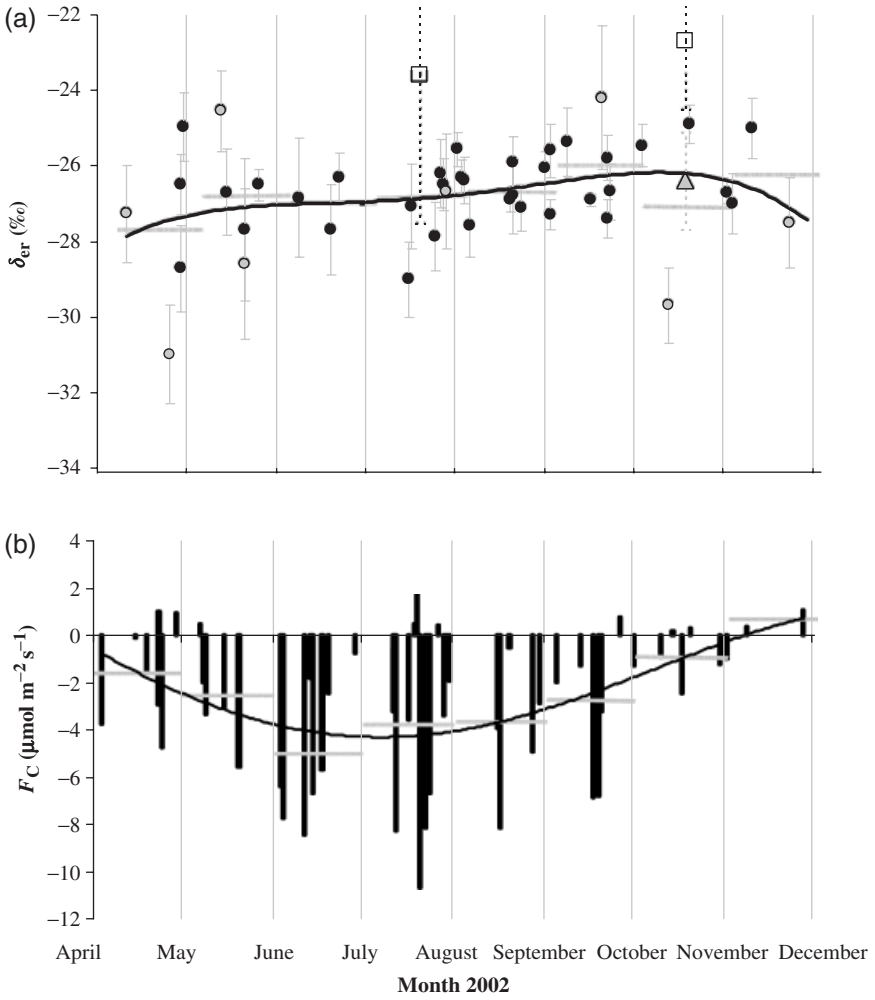

Fig. 6 2002 seasonal variations in (a) $\delta^{13}C$ of ecosystem respired CO_2, δ_{er} (circles) and (b) 24 h averaged (00:00–23:30 hours on the air sampling day) net ecosystem exchange, NEE (bars). Grey circles highlight δ_{er} values estimated with [CO_2] ranges <30 ppm (not used in data analysis; see Method for details). Error bars delimit the standard error (SE) of the δ_{er} estimate. Horizontal stippled lines are monthly average values and thick black lines represent 3rd-order polynomial fits. Large symbols (dashed lines for SE) show the δ_{er} values estimated from air sampled at two NOAA/CMDL network stations, Mace Head, Ireland (grey triangles) and Hegyhatsal, Hungary (open squares), between June–August and September–November. Data for June–August at Mace Head were missing. Gridlines highlight the 1st day of each month. Note that November and December are omitted from the smoothed line fit because these values are generally for sites where seasonal photosynthetic activity is largest during winter, as such their seasonal trends could be expected to be different from results from the other sites.

in August and September, when 2001 values were 1.7‰ and 2.1‰ higher, respectively, than corresponding 2002 values.

During July and August, significant longitudinal (but no latitudinal) trends were observed in the 2001, and most of the 2002, δ_{er} values (Fig. 7). For both years, δ_{er} was generally enriched in sites located further eastwards (inland), and in 2001, the slope of this longitudinal change was considerably steeper (0.18‰°E^{-1}) than in 2002 (0.04‰°E^{-1}). Consequently, in 2001 δ_{er} values were up to 3.0‰ more enriched at sites between 10.0°E and 13.5°E compared with the same sites in 2002, while in the more western sites δ_{er} values were similar in both years. This longitudinal relationship did not hold for certain specific sites, (i.e. Hyytiälä, Finland in 2002) and during other time periods, which indicates that it is likely an indirect effect, probably of site meteorology. Indeed, large spatial and temporal meteorological gradients existed across the network sites (Table 3). In addition to the typical radiation-driven north to south increase in mean annual air temperature (T_a), which ranged from −1.0 °C in Sodankylä, northern Finland to + 22.0 °C in Yatir, Israel, there was a significant continental effect (Lindner *et al.*, 1996)

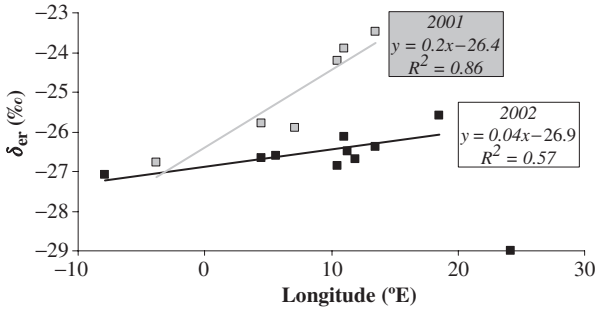

Fig. 7 Longitudinal trends in the $\delta^{13}C$ of ecosystem respired CO_2, δ_{er}, in 2001 (grey squares) and 2002 (black squares). All values are site averages for July and August. Linear regression lines and equations are shown for each year, with one point excluded ($\delta_{er} = -29‰$ for Hyytiälä, Finland in 2002).

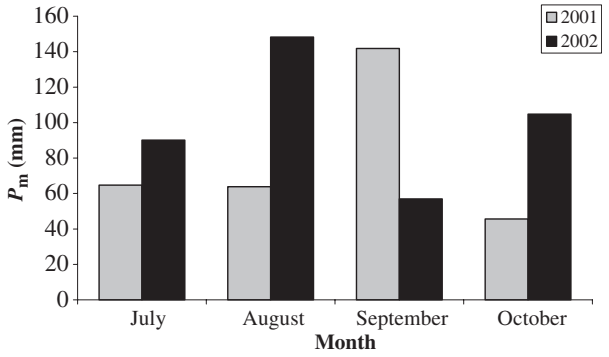

Fig. 8 Average monthly precipitation, P_m, for sites sampled during the common sampling period (July–October) in 2001 and 2002.

observed in the temperature and precipitation records; more easterly locations generally experienced warmer, drier climates during the summer months and a larger annual temperature range. Precipitation varied considerably across the network, from ~ 1200 mm per annum in Griffin, Scotland to ~ 275 mm in Yatir, Israel, with drier sites tending to be located further south.

As with the observed spatial gradients in δ_{er}, longitudinal variations in meteorological parameters were generally largest during the summer months (July and August), when the (temperature and humidity) continentality effect was most pronounced (Oliver & Fairbridge, 1987). In 2001, significant longitudinal relationships were noted with daytime averaged vapor pressure deficit (VPD) (VPD = 0.04°E + 0.6, $R^2 = 0.79$, $P < 0.01$), relative humidity (RH) (RH = −1.2°E + 73.7, $R^2 = 0.65$, $P < 0.01$) and T_a ($T_a = 0.4$°E + 18.0, $R^2 = 0.58$, $P < 0.01$), yet in 2002, no significant meteorological trends were observed with longitude. Before July and after late-August, differences in VPD, RH and T_a between the more maritime, western, and continental, eastern, locations were relatively small, and their longitudinal trends insignificant. Monthly average precipitation, P_m, showed no significant longitudinal relationships in either year (data not shown).

The close association between meteorological conditions during July–August and corresponding δ_{er} values was clearly evident in the two study years. In 2001, July and August δ_{er} values were significantly related with daytime averaged VPD ($\delta_{er} = 3.0$VPD−27.7, $R^2 = 0.47$, $P < 0.01$), RH ($\delta_{er} = -0.1$RH−18.6, $R^2 = 0.43$, $P < 0.01$), less so with T_a ($\delta_{er} = 0.23T_a - 29.8$, $R^2 = 0.33$, $P < 0.01$), and not significantly with P_m. In contrast, in 2002, δ_{er} was significantly related with T_a ($\delta_{er} = 0.08T_a - 28.2$, $R^2 = 0.76$, $P < 0.01$) and P_m ($\delta_{er} = 0.005P_m - 27.1$, $R^2 = 0.54$, $P < 0.01$), but insignificantly with VPD and RH. These relationships appear to be related with the timing and quantity of precipitation during this period because, while the July–August average T_a, VPD and RH values across the sampled sites were not significantly different between 2001 and 2002, P_m in 2002 was nearly double the 2001 average (Fig. 8). This enhanced precipitation was a large-scale phenomenon (resulting in major floods in eastern Europe) and was noted in the Brasschaat, Belgium, Nonantola, Italy and Tharandt, Germany sites. Notably, in September, after the peak activity period, no significant relationships were observed between δ_{er} and T_a or P_m, even though P_m during this month was twice as large in 2001 than in 2002.

The possibility of time-lags existing between a meteorological change and the δ_{er} response was examined by using VPD, RH and T_a data measured at each site's flux tower and recorded as 30 min averages. These meteorological data were averaged over various time windows (3, 6, 9 and 12 h) and lagged backwards in 30 min steps, where the first time step was for the period 6 h prior to 18:00 hours on the sampling day (zero lag time) and the last ended exactly 12 days prior. At each step, correlations were made between δ_{er} and each meteorological parameter. Six hours average meteorological parameters generally displayed the most significant correlations with δ_{er}, although similar features were observed with all time windows. In 2001, clear diurnal cycles were noted in these correlations which persisted from up to 7 days prior to sampling (Fig. 9a). The most significant correlations ($P < 0.01$) were noted (1) between δ_{er} and both VPD and RH during mid-day ($\pm$ 3 h) on the day prior to the night air sampling, (2) with RH at both 2 and 6 days time lag, and (3) with VPD at 6 days lag. In contrast, for the same time period in 2002 (July–November) there were no consistent cycles in the correlations, and significant correlations ($P < 0.01$) were only noted between δ_{er} and

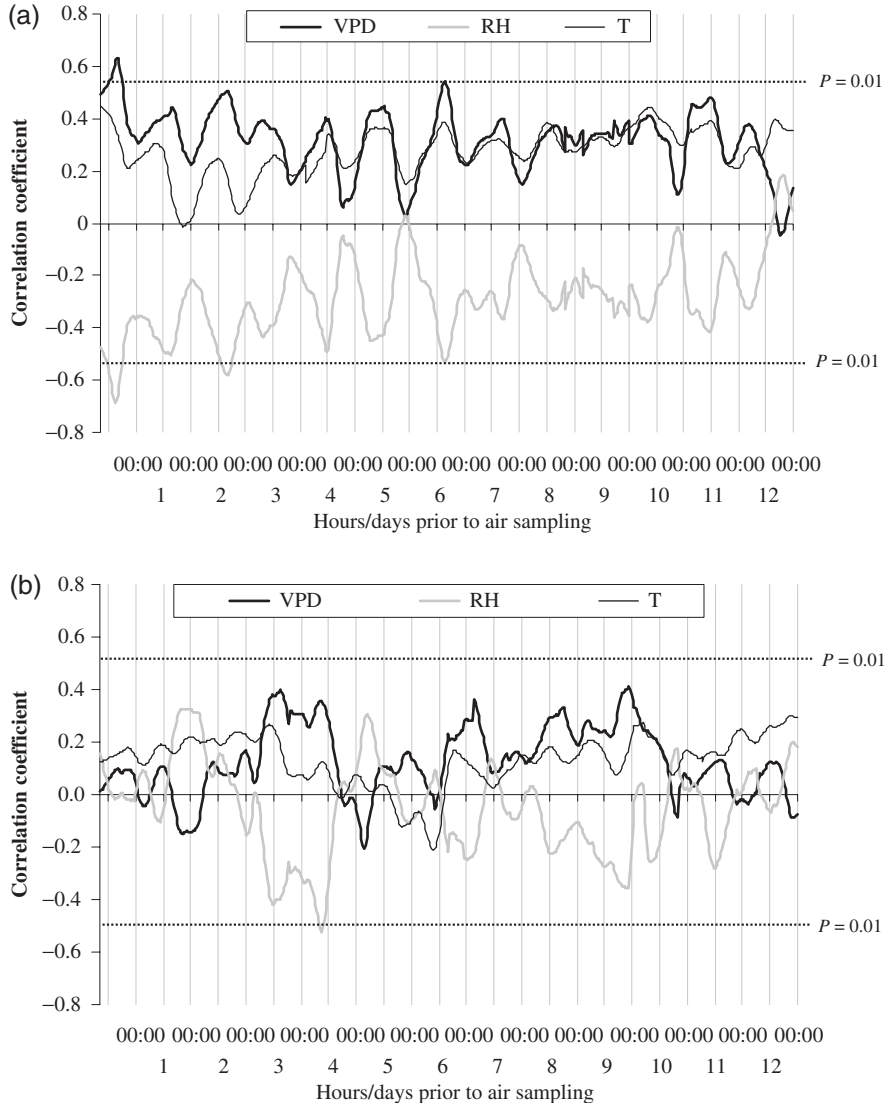

Fig. 9 Running mean correlation between δ_{er} and vapor pressure deficit (VPD), relative humidity (RH) and air temperature (T_a) for sampling campaigns between July and October 2001 (a) and 2002 (b). Each correlation coefficient series corresponds to the correlation between the δ_{er} for all sampling campaigns and a corresponding 6 h average of each environmental parameter, with different lag times, in 30 min time steps from 18:00 hours on the day of sampling to 12 days prior to sampling. Vertical lines indicate 12-h time steps and δ the day indicator is at mid-day. Horizontal dotted lines delimit significance of correlation coefficients where $P = 0.01$.

RH 3 days prior to sampling (Fig. 9b). Correlations between δ_{er} and T_a were not significant at any time lag during 2001 or 2002.

Relationships between δ_{er} and net ecosystem CO_2 exchange (NEE)

During 2001, the seasonal trend in δ_{er} was generally mirrored by variations in the 24 h average (00:00–23:30 hours), NEE, at each site on the specific sampling days (Fig. 5). Note that negative NEE values refer to net CO_2 uptake by the forest ecosystem, and *vice versa*. The observed increase in δ_{er} during July 2001 was accompanied by a rapid increase in net CO_2 uptake from NEE values around $-1.5\,\mu mol\,m^{-2}\,s^{-1}$ to $-8.0\,\mu mol\,m^{-2}\,s^{-1}$. Uptake remained relatively high (between -2.0 and $-5.0\,\mu mol\,m^{-2}\,s^{-1}$) throughout August and September, then decreased rapidly, with decreasing δ_{er}, through October. Despite the apparent seasonal relationship between δ_{er} and NEE in 2001, regression analyses showed no consistent relationships between these data sets. Significantly, during the periods of highest net CO_2 uptake, NEE $< -2.0\,\mu mol\,m^{-2}\,s^{-1}$, which comprised over 80% of the total NEE on study days, δ_{er} values

were rather insensitive to variations in NEE, but were on average 1.5‰ higher in 2001, -25.0 ± 1.1‰, than in 2002, -26.5 ± 1.1‰. This isotopic difference was not associated with a difference in NEE.

$\delta^{13}C$ of organic matter

Annual average $\delta^{13}C$ values of bulk leaf, $\delta^{13}C_L$, stem, $\delta^{13}C_{St}$, soil, $\delta^{13}C_{So}$ and root, $\delta^{13}C_{Rt}$ organic matter ranged between -22.2‰ and -32.1‰ in 2001, and -22.0‰ and 33.5‰ in 2002. In both years, there was an average enrichment in ^{13}C, of ~ 2.0‰, in going from $\delta^{13}C_L$, through $\delta^{13}C_{St}$ to $\delta^{13}C_{So}$ or $\delta^{13}C_{Rt}$ (Table 4).

There were no clear seasonal or spatial trends in any of the organic matter $\delta^{13}C$ series, although, for some tree species there were consistent and significant differences between $\delta^{13}C_L$ and $\delta^{13}C_{So}$, both in 2001 and 2002 (Fig. 10). At sites dominated by angiosperms; *Fagus sylvatica* or *Quercus robur/Fraxinus* spp., there were significant average differences between $\delta^{13}C_L$ and $\delta^{13}C_{So}$ (up to 4.4‰ for *Fagus sylvatica*). However, at other sites dominated by gymnosperms, no clear differences between $\delta^{13}C_L$ and $\delta^{13}C_{So}$ occurred. It was noted at least in one site (Hainich) that depleted $\delta^{13}C_L$ values may have been because of the low sampling height (~ 2 m) because large gradients in $\delta^{13}C_L$ (~ 6.0‰) between upper and lower canopy at this site (Knohl *et al*., 2005). The *Pinus halepensis* dominated forest at Yatir, Israel, was an exception to all other observations because it was the only site where $\delta^{13}C_L$ values were consistently enriched, by ~ 2.0‰, compared with corresponding $\delta^{13}C_{So}$ values.

Significant relationships between prevailing climatic conditions and the $\delta^{13}C$ of leaf and stem (tree ring) material are commonly observed over time within the same tree and spatially across climate gradients (Saurer & Siegenthaler, 1989; Loader *et al*., 1995; Robertson *et al*., 1997; Switsur & Waterhouse, 1998). However, no such relationships between bulk material $\delta^{13}C$ values and meteorology were noted across network sites, even when meteorological data from each site were averaged for various time periods up to 3 months prior to the sampling date, or when individual site or species data were considered.

Potential for partitioning ecosystem respiration

The isotopic composition of ecosystem components has been proposed as a powerful means for partitioning ecosystem CO_2 fluxes into autotrophic and heterotrophic (Högberg *et al*., 2001; Ogee *et al*., 2004), or below- and aboveground fluxes (Yakir & Sternberg, 2000). We tested the potential for such partitioning within the framework of the network $\delta^{13}C$ results.

Assuming that δ_{er} for all sampling campaigns was composed of two predominant components, autotrophic (au) and heterotrophic (h) and the CO_2 added by respiration, c_{er}, to the nocturnal canopy air is only composed of these two sources (i.e., $c_{er} = c_{au} + c_h$), the following isotopic mass balance applies:

$$c_{er}\delta_{er} = c_{au}\delta_{au} + c_h\delta_h, \quad (6)$$

where, the concentration-weighted signal of respired CO_2 equals the sum of autotrophic and heterotrophic isotopic signals, weighted by their respective concentrations. Here, we used local δ_{er} values from the network data set, and solved for the relative autotrophic and hererotrophic contributions (autotrophic flux, $f_{au} = c_{au}/c_{er}$, and hererotrophic flux, $f_h = 1 - f_{au}$). The δ_{au} and δ_h values were assumed to be represented by $\delta^{13}C_L$ and $\delta^{13}C_{So}$, respectively. Provided the values of δ_{au} and δ_h were distinct, relative contributions of the two respiratory components, f_{au} and f_h, could be derived.

It was immediately clear from the estimates of δ_{er} compared with $\delta^{13}C_L$ and $\delta^{13}C_{So}$ values that this approach was not applicable. Often values of $\delta^{13}C_L$ and $\delta^{13}C_{So}$ did not envelope the corresponding δ_{er} values as one would expect. This was also the case with the monthly averages, (e.g. the average network δ_{er} for August 2001 was -25.2‰ and for September -24.7‰ δ, yet both corresponding $\delta^{13}C_L$ and $\delta^{13}C_{So}$ values were at least 1.6‰ less enriched). On most occasions, to balance the δ_{er} values, contributions from unaccounted–for sources of higher $\delta^{13}C$ would be required, or the assumptions underlying this approach were flawed.

Regional-scale $\delta^{13}C$ signatures

To compare our local ecosystem estimates of δ_{er} with regional-scale atmospheric $\delta^{13}C$ signals (see Figs 5 and 6), Eqn (3) was applied to $[CO_2]$ and $\delta^{13}C$ results from air samples collected at two European NOAA-CMDL background stations (Mace Head, Ireland, and Hegyhatsal, Hungary) (Bakwin *et al*., 1998; Miller & Tans, 2003). Utilizing these, usually fortnightly, observations, regional-scale $\delta^{13}C$ signals were estimated for two time periods; summer, June–August, and autumn, September–November. To account for the changing $\delta^{13}C$ of background CO_2 over these periods, seasonal trends in both the $[CO_2]$ and $\delta^{13}C$ data were first removed using 3rd order polynomial trend lines (see Fig. 3), and Eqn (3) was applied to the residual, detrended values. Regression analyses and the treatment of outliers were the same as for estimation of δ_{er} (see Methods). The resulting estimates of $\delta^{13}C$ provide an indication of the dominant $\delta^{13}C$ signature of regional-scale CO_2 sources and sinks over the 3-month periods (Table 5).

Table 4 The $\delta^{13}C$ of leaf, $\delta^{13}C_L$, stem, $\delta^{13}C_{St}$, soil, $\delta^{13}C_{So}$, and root, $\delta^{13}C_{Rt}$, organic matter from 2001 and 2002 sampling campaigns

Site	Sampling date	$\delta^{13}C_L$ (‰)	$\delta^{13}C_{St}$ (‰)	$\delta^{13}C_{So}$ (‰)	$\delta^{13}C_{Rt}$ (‰)
2001					
Brasschaat, Belgium	02/07/01	−28.0	−27.6	−27.1	−26.6
Brasschaat, Belgium	03/07/01	−28.0	n/a	−27.7	−26.5
Griffin, Scotland	03/07/01	−29.4	−27.6	−29.5	n/a
Griffin, Scotland	09/07/01	−29.2	−28.2	−28.8	−29.1
Nonantola, Italy	10/07/01	−28.1	−28.3	−26.1	−25.1
Hainich, Germany	24/07/01	−30.0	−32.1	−25.8	−26.8
Hesse, France	25/07/01	−29.6	−28.6	−25.4	n/a
Hainich, Germany	02/08/01	−29.7	n/a	−25.2	−25.7
Tharandt, Germany	12/08/01	−26.6	−23.2	−26.3	n/a
Griffin, Scotland	13/08/01	−30.1	−28.2	−29.1	n/a
Tharandt, Germany	14/08/01	−26.1	−25.1	−25.8	n/a
Brasschaat, Belgium	28/08/01	−28.4	−27.6	−26.8	−26.9
Brasschaat, Belgium	29/08/01	−28.4	−27.1	−27.8	−27.0
Griffin, Scotland	10/09/01	−28.3	−27.4	−29.2	n/a
Nonantola, Italy	20/09/01	−29.0	−28.1	−26.0	−24.9
Yatir, Israel	20/09/01	−23.1	−22.2	−24.8	−24.0
Hainich, Germany	25/09/01	−30.3	−32.1	−25.2	−24.7
Tharandt, Germany	07/10/01	−26.6	−24.5	−26.2	n/a
Hyytiälä, Finland	09/10/01	−26.3	−25.3	−26.8	n/a
Tharandt, Germany	11/10/01	−26.6	−24.6	−26.5	n/a
LooBos, Netherlands	16/10/01	−29.4	−28.0	−24.0	−25.8
Collelongo, Italy	18/10/01	−28.5	−25.6	−25.3	n/a
Hainich, Germany	18/10/01	−30.2	−30.3	−24.5	−25.7
Nonantola, Italy	30/10/01	−28.9	−26.6	−26.7	−26.1
Le Bray, France	31/10/01	−28.2	−27.7	−27.6	n/a
Brasschaat, Belgium	01/11/01	−28.7	−27.5	−28.0	n/a
Brasschaat, Belgium	05/11/01	−29.1	−28.0	−27.9	n/a
Bily Kriz, Czech Rep.	06/11/01	−29.0	−28.0	−26.6	n/a
Le Bray, France	07/11/01	−28.1	−30.1	−27.3	n/a
Bily Kriz, Czech Rep.	13/11/01	−28.4	−27.2	−27.1	n/a
Yatir, Israel	20/11/01	−22.3	−22.2	−24.8	−24.0
Collelongo, Italy	26/11/01	−28.7	−27.0	−24.9	n/a
Evora, Portugal	04/12/01	−27.6	−26.2	−27.8	n/a
2001 average		−28.1	−27.2	−26.6	−25.9
Standard deviation		1.8	2.4	1.4	1.3
2002					
Tharandt, Germany	04/04/02	−26.6	−25.5	−26.6	n/a
Yatir, Israel	15/04/02	−23.6	−22.2	n/a	n/a
Evora, Portugal	19/04/02	−27.9	−27.1	−27.5	n/a
LooBos, Netherlands	23/04/02	−29.2	−27.4	−27.7	n/a
Soroe, Denmark	23/04/02	−30.6	−31.1	−26.5	n/a
Collelongo, Italy	29/04/02	−24.7	−26.6	−26.1	n/a
Bily Kriz, Czech Rep.	07/05/02	−28.6	n/a	−26.1	n/a
Brasschaat, Belgium	08/05/02	−29.0	−28.6	−27.8	n/a
LooBos, Netherlands	09/05/02	n/a	n/a	n/a	n/a
Hainich, Germany	15/05/02	−31.3	−32.2	−26.1	−25.1
Bily Kriz, Czech Rep.	15/05/02	−27.5	n/a	−25.9	n/a
Yatir, Israel	15/05/02	−23.9	−22.0	n/a	n/a
Nonantola, Italy	20/05/02	−28.5	−27.0	−24.2	n/a
Tharandt, Germany	03/06/02	−27.9	−24.4	−26.9	n/a
Soroe, Denmark	04/06/02	−31.6	−32.0	−27.2	n/a

(continued)

Table 4 (Contd.)

Site	Sampling date	$\delta^{13}C_L$ (‰)	$\delta^{13}C_{St}$ (‰)	$\delta^{13}C_{So}$ (‰)	$\delta^{13}C_{Rt}$ (‰)
Collelongo, Italy	11/06/02	−27.5	−26.7	−26.0	n/a
Hainich, Germany	13/06/02	−31.6	−30.9	−27.8	−28.3
Hesse, France	14/06/02	−27.8	−26.2	−26.2	n/a
Nonantola, Italy	17/06/02	−28.8	−26.6	−25.4	−26.6
Bily Kriz, Czech Rep.	19/06/02	−27.3	n/a	−27.0	n/a
Evora, Portugal	28/06/02	−27.7	−26.9	−26.6	n/a
Hyytiälä, Finland	11/07/02	−26.6	n/a	−27.3	n/a
Dooary, Ireland	12/07/02	−29.8	n/a	n/a	−28.1
Yatir, Israel	18/07/02	−22.7	−22.0	n/a	n/a
Hainich, Germany	20/07/02	−32.9	−26.5	−26.4	−27.6
Nonantola, Italy	22/07/02	−29.2	−28.4	−26.6	n/a
Hesse, France	22/07/02	−28.4	−26.0	−26.0	n/a
Lavarone, Italy	23/07/02	−25.7	−25.5	−24.7	n/a
Collelongo, Italy	24/07/02	−27.8	−26.2	−25.9	n/a
Le Bray, France	26/07/02	−29.7	−29.7	−27.4	n/a
Brasschaat, Belgium	28/07/02	−28.8	−27.9	−28.0	n/a
LooBos, Netherlands	29/07/02	−27.9	−25.9	−27.9	n/a
Tharandt, Germany	30/07/02	−27.9	−25.1	−26.3	n/a
Sodankyla, Finland	01/08/02	−29.2	−27.6	−27.3	n/a
Hainich, Germany	16/08/02	−32.4	−33.2	−24.7	−25.2
Soroe, Denmark	16/08/02	−32.1	n/a	−26.8	n/a
Brasschaat, Belgium	19/08/02	−29.5	−28.7	−27.8	n/a
Collelongo, Italy	21/08/02	−27.7	−25.0	−26.2	n/a
Nonantola, Italy	27/08/02	−31.2	−28.6	−26.3	−26.1
Bily Kriz, Czech Rep.	29/08/02	−29.1	n/a	−26.5	n/a
Dooary, Ireland	04/09/02	−32.3	n/a	−29.0	n/a
Hyytiälä, Finland	12/09/02	−27.1	n/a	−27.4	n/a
Hainich, Germany	16/09/02	−32.2	−32.8	−26.9	−25.9
Tharandt, Germany	19/09/02	−26.7	−25.2	−25.8	n/a
Evora, Portugal	25/09/02	−27.4	−25.8	−24.5	n/a
Collelongo, Italy	27/09/02	−28.1	−24.9	−25.3	n/a
Nonantola, Italy	30/09/02	−30.1	−28.2	−27.4	−25.6
Brasschaat, Belgium	09/10/02	−29.3	−28.7	−28.4	n/a
Soroe, Denmark	09/10/02	−33.5	n/a	n/a	n/a
Brasschaat, Belgium	13/10/02	−28.5	−28.1	−27.7	n/a
Lavarone, Italy	16/10/02	−28.7	−24.1	−26.9	n/a
Hainich, Germany	19/10/02	−32.9	−23.4	−28.2	−28.5
Tharandt, Germany	29/10/02	−27.0	−23.9	−24.6	n/a
LooBos, Netherlands	31/10/02	−28.5	−26.3	−28.4	n/a
Nonantola, Italy	07/11/02	−29.6	−27.7	−26.9	−26.3
Collelongo, Italy	20/11/02	n/a	−25.9	−26.5	−26.9
Evora, Portugal	03/12/02	−27.7	−28.0	−29.6	n/a
Yatir, Israel	15/01/03	−23.4	n/a	n/a	n/a
2002 average		−28.6	−27.0	−26.7	−26.7
Standard deviation		2.4	2.7	1.2	1.2

Annual averages and standard deviations are listed at the base of each years' data. n/a means data not available.

For 2001, the regional $\delta^{13}C$ signature in summer and autumn was $\sim$1.0‰ more enriched at Mace Head, Ireland (−23.2‰ and −25.1‰) than at Hegyhatsal, Hungary (−24.4‰ and −26.7‰), and both sites showed $\sim$2.0‰ more enriched signals in summer than in autumn (Table 5). During 2002, the summer and autumn $\delta^{13}C$ signatures at Hegyhatsal were >1.5‰ more enriched than corresponding 2001 data, and, unlike 2001, the autumn value was slightly enriched (−22.7‰) compared with the summer (−23.6‰). In

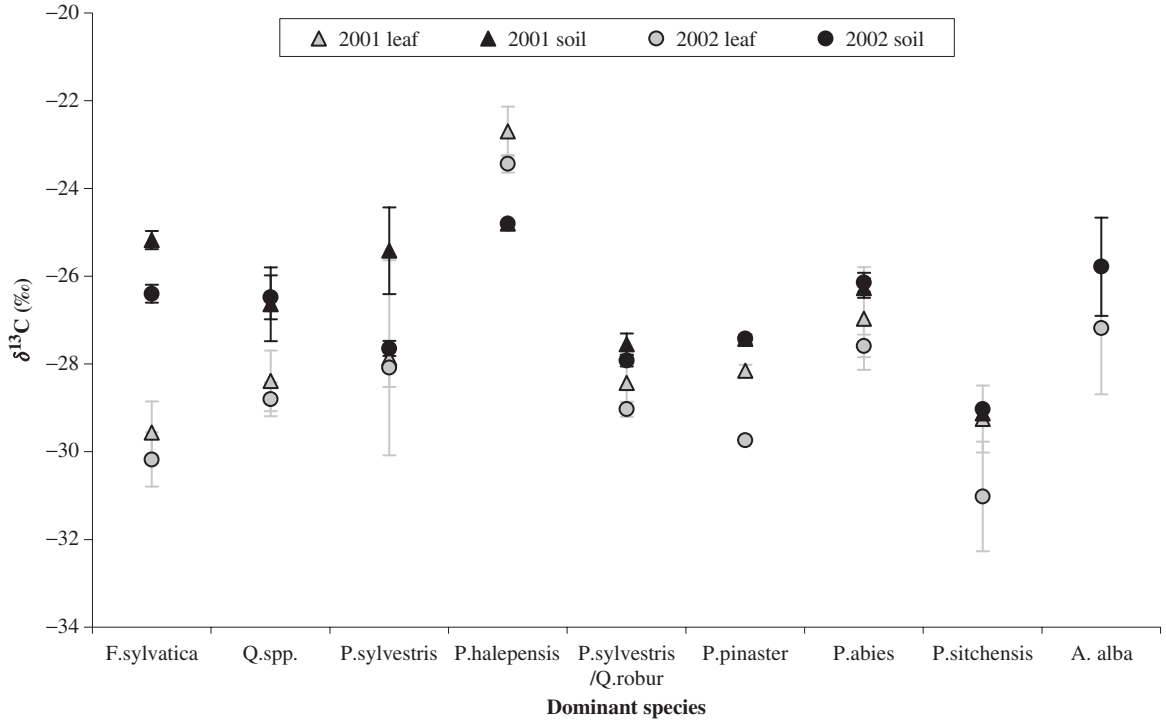

Fig. 10 Average and standard error (SE) of leaf (grey symbols) and soil (black symbols) organic matter $\delta^{13}C$ in 2001 (triangles) and 2002 (circles) for dominant species across the network sites. See Table 4 for individual site and species details.

comparison, the autumn $\delta^{13}C$ signature at Mace Head was similar to values observed for 2001 (−26.4‰), although, the difference between stations and seasons could not be examined at this site because of missing data during the summer period.

Ecosystem respiration 'discrimination'

Converting δ_{er} to estimates of 'discrimination' associated with ecosystem respiration, Δ_{er}, takes into account variations in δ_a and is often used in regional and global budget estimates (Eqn (1), see Introduction). Strictly, from the derivation in Eqns (2) and (3), δ_a is the initial $\delta^{13}C$ value of atmospheric CO_2 into which δ_{er} is mixed and, δ_a and c_a will necessarily define some point along the Keeling plot mixing line. In this sense, given that δ_{er} in our forest ecosystems is always more negative than the $\delta^{13}C$ of tropospheric air, δ_a could be any value on the mixing line provided it is between the $\delta^{13}C$ of night-time canopy air samples and the $\delta^{13}C$ of air above the planetary boundary layer. Although the specific value of δ_a is not important for computing δ_{er}, it is clear that the scale and timing chosen to define δ_a will directly influence the resulting Δ_{er} values, and therefore their interpretation. Considering this direct influence of δ_a on estimations of Δ_{er}, we chose to examine the sensitivity of Δ_{er} to three different methods of estimating δ_a (see Methods). This comparison was completed only on the 2001 data. Nevertheless, the results are valuable for the interpretation of all Δ_{er} data, because they demonstrate the scale of Δ_{er} differences that can be expected given different assumptions regarding δ_a. They also highlight some of the key conceptual and procedural difficulties involved with the estimation of discrimination values that are representative of the net ecosystem $\delta^{13}C$ signal.

Of the three techniques used to estimate δ_a, Methods 1 and 2 utilized the slope method regression equations for each site and sampling period, whereas Method 3 used a single record of δ_a from Hegyhatsal, Hungary to represent all sites. It was expected that δ_a estimates from Methods 1 and 2 would be more intimately linked with the localized ecosystem conditions than those of Method 3. Indeed, δ_a and subsequent Δ_{er} values calculated using Methods 1 and 2 were very similar, and these differed by up to 2.2‰ from the Method 3 estimates, with the largest differences occurring during the most active summer months (Table 6, Fig. 11b). Although the choice of δ_a values clearly has a significant influence on the spatial and temporal variations in estimated Δ_{er}, it is not obvious which δ_a method, the more locally- or regionally relevant, is preferable or more applicable. We arbitrarily chose to use the Method 3 estimates of δ_a to calculate Δ_{er} for

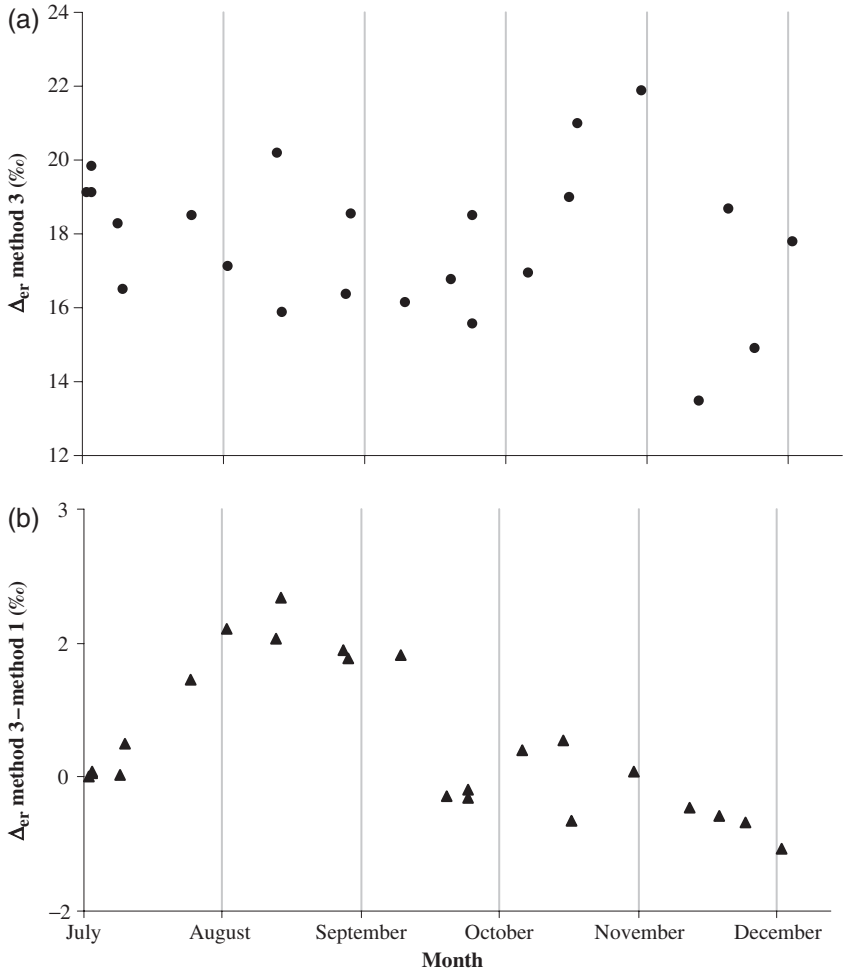

Fig. 11 (a) Values of Δ_{er} for 2001 calculated using $\delta^{13}C$ of background air, δ_a, values estimated using Method 3 (see text for details), and (b) Difference between Δ_{er} calculated using δ_a values estimated with Method 3 minus those with Method 1. Note, Methods 3 and 1 showed the largest differences. Tick marks on the *x*-axis are on the 1st day of the month.

Table 5 Details of regression lines (slope = δ_e; Eqn (4)) of atmospheric $[CO_2]$ versus $[CO_2]\cdot\delta^{13}C$ data from two NOAA/CMDL background stations in Europe: Mace Head, Ireland and Hegyhatsal, Hungary

Site	Year	Period	Equation	R^2	SE (‰)
Mace Head, Ireland	2001	June–Aug	$y = -23.2x - 2.0$	0.91	2.5
Mace Head, Ireland	2001	Sept–Nov	$y = -25.1x + 1.7$	0.98	1.1
Hegyhatsal, Hungary	2001	June–Aug	$y = -24.4x - 13.8$	0.96	1.9
Hegyhatsal, Hungary	2001	Sept–Nov	$y = -26.7x + 22.4$	0.95	2.1
Mace Head, Ireland	2002	Sept–Nov	$y = -26.4x - 3.0$	0.99	1.3
Hegyhatsal, Hungary	2002	June–Aug	$y = -23.6x + 26.4$	0.86	3.9
Hegyhatsal, Hungary	2002	Sept–Nov	$y = -22.7x + 19.2$	0.94	1.8

Data are separated into two time periods: June-August and September–November. Seasonal trends in both the $[CO_2]$ and $\delta^{13}C$ data were first removed using 3rd order polynomial trend lines (see Fig. 3), and Eqn (4) was applied to the residual values. Results for Mace Head in June-August 2002 were omitted because of missing data. The R^2 of the regression line and SE of the slope are listed.

both 2001 and 2002, and this is consistent with other recent large-scale network studies of 'ecosystem discrimination' (e.g. Buchmann & Kaplan 2001; Lai *et al*., 2004). It must be remembered that this definition of Δ_{er} neglects spatial variations in δ_a and indicated only general seasonal $\delta^{13}C$ trends reflected in the regional atmospheric station. Despite this somewhat arbitrary assignment of Δ_{er}, it was reassuring to note that the

Table 6 2001 data from three methods of estimating the $\delta^{13}C$ composition of background air (δ_a) and subsequent ecosystem respiration 'discrimination' (Δ_{er}, see Introduction) values for each sampling event (see text for details)

		Method 1		Method 2		Method 3	
Site	Date	δ_a (‰)	Δ_{er} (‰)	δ_a (‰)	Δ_{er} (‰)	δ_a (‰)	Δ_{er} (‰)
Brasschaat, Belgium	02/07/01	−7.8	19.1			−8.2	18.6
Brasschaat, Belgium	03/07/01	−7.9	19.0			−8.3	18.6
Griffin, Scotland	03/07/01	−7.9	19.8	−8.0	19.7	−8.3	19.4
Griffin, Scotland	09/07/01	−7.8	18.2	−8.0	18.1	−8.3	17.7
Nonantola, Italy	10/07/01	−8.2	16.1			−8.3	15.9
Hesse, France	25/07/01	−9.0	17.3			−8.5	17.8
Hainich, Germany	02/08/01	−9.7	15.3	−8.8	16.2	−8.6	16.4
Griffin, Scotland	13/08/01	−9.7	18.4			−8.7	19.4
Tharandt, Germany	14/08/01	−10.2	13.6			−8.7	15.1
Brasschaat, Belgium	28/08/01	−9.6	14.8	−9.8	14.7	−8.8	15.7
Brasschaat, Belgium	29/08/01	−9.6	17.1	−9.8	16.9	−8.8	17.9
Griffin, Scotland	10/09/01	−9.7	14.6			−8.9	15.5
Nonantola, Italy	20/09/01	−8.1	17.0			−8.9	16.2
Hainich, Germany	25/09/01	−8.1	18.7			−8.9	18.0
Loobos, Netherlands	25/09/01	−8.3	15.7			−8.9	15.1
Tharandt, Germany	07/10/01	−8.9	16.6			−8.9	16.5
Loobos, Netherlands	16/10/01	−9.0	18.5			−8.9	18.7
Hainich, Germany	18/10/01	−8.1	21.5			−8.9	20.7
Brasschaat, Belgium	01/11/01	−8.8	21.8			−8.8	21.9
Bily Kriz, Czech Republic	13/11/01	−8.5	13.8			−8.7	13.6
Yatir, Israel	20/11/01	−8.5	19.2			−8.7	18.9
Collelongo, Italy	26/11/01	−8.4	15.4			−8.7	15.2
Evora, Portugal	04/12/01	−8.1	18.6			−8.7	18.1
2001 average		−8.7	17.4	−8.9	17.1	−8.4	17.8
Tharandt, Germany	04/04/02					−8.5	19.3
Evora, Portugal	19/04/02					−8.4	23.3
LooBos, Netherlands	23/04/02					−8.3	18.7
Soroe, Denmark	23/04/02					−8.3	21.0
Dooary, Ireland	24/04/02					−8.3	17.1
Bily Kriz, Czech Rep.	07/05/02					−8.2	16.8
LooBos, Netherlands	09/05/02					−8.2	19.0
Hainich, Germany	15/05/02					−8.1	20.1
Yatir, Israel	15/05/02					−8.1	21.1
Nonantola, Italy	20/05/02					−8.1	18.9
Tharandt, Germany	03/06/02					−8.0	19.4
Hesse, France	14/06/02					−7.9	20.3
Nonantola, Italy	17/06/02					−7.9	18.9
Hyytiälä, Finland	11/07/02					−7.8	21.8
Dooary, Ireland	12/07/02					−7.8	19.8
Hainich, Germany	20/07/02					−7.8	20.7
Nonantola, Italy	22/07/02					−7.8	18.9
Lavarone, Italy	23/07/02					−7.8	19.2
Collelongo, Italy	24/07/02					−7.8	19.4
Brasschaat, Belgium	28/07/02					−7.8	18.2
LooBos, Netherlands	29/07/02					−7.8	19.0
Tharandt, Germany	30/07/02					−7.8	19.1
Sodankyla, Finland	01/08/02					−7.8	20.4
LooBos, Netherlands	15/08/02					−7.8	19.6
Hainich, Germany	16/08/02					−7.8	18.6
Soroe, Denmark	16/08/02					−7.8	19.5
Brasschaat, Belgium	19/08/02					−7.8	19.8

(continued)

Table 6 (Contd.)

		Method 1		Method 2		Method 3	
Site	Date	δ_a (‰)	Δ_{er} (‰)	δ_a (‰)	Δ_{er} (‰)	δ_a (‰)	Δ_{er} (‰)
Nonantola, Italy	27/08/02					−7.9	18.7
Brasschaat, Belgium	29/08/02					−7.9	20.0
Bily Kriz, Czech Rep.	29/08/02					−7.9	18.2
Dooary, Ireland	04/09/02					−7.9	17.9
Hyytiälä, Finland	12/09/02					−8.0	19.5
Hainich, Germany	16/09/02					−8.0	16.6
LooBos, Netherlands	18/09/02					−8.0	19.9
Lavarone, Italy	18/09/02					−8.0	18.2
Tharandt, Germany	19/09/02					−8.0	19.2
Nonantola, Italy	30/09/02					−8.1	17.8
Lavarone, Italy	16/10/02					−8.3	17.0
Tharandt, Germany	29/10/02					−8.5	18.7
LooBos, Netherlands	31/10/02					−8.5	19.0
Nonantola, Italy	07/11/02					−8.6	16.8
Collelongo, Italy	20/11/02					−8.8	19.3
2002 average						−8.1	19.0

Estimates are made only for samplings when the SE of δ_{er} was <2.0‰.

general spatial and temporal trends in Δ_{er} were consistent, regardless of the method used to estimate δ_a (to a large extent because variations in δ_{er} were much larger than in δ_a). This provides confidence that these trends are relatively robust.

Using δ_a values estimated with Method 3, average Δ_{er} values for 2001 and 2002 were 17.8 ± 2.0‰ and 19.0 ± 1.6‰, respectively. As with δ_{er}, average July to November Δ_{er} for 2002 was the same as the whole season average, confirming that the difference observed between 2001 and 2002 was not a function of different sampling sites and durations. The full range of Δ_{er} values was between 13.5‰ and 21.9‰ in 2001, and 14.2‰ and 23.3‰ in 2002, although, during the periods of peak activity (most negative NEE), the variations in Δ_{er} were relatively conservative, typically between 15.0‰ and 19.0‰. Fluctuations in δ_{er} were almost exactly mirrored by Δ_{er}, because of the fact that δ_a was assumed to be spatially constant across the network, and its seasonal variability was small (≤ 0.6‰) relative to δ_{er} (Table 3). As a result, the significant spatial, temporal and meteorological relationships noted with δ_{er} also apply, inversely, to Δ_{er}. For brevity, these relationships are not reported separately here.

Discussion

A major advantage of global-scale atmospheric budget studies, including CO_2, is that they deal with an essentially closed system where an annual balance is a clear constraint. However, such budgets are not sufficient to identify the sinks and sources to and from the land biosphere, or the processes that influence them. Ecosystem-scale studies are required, but these introduce extensive heterogeneity and high levels of complexity that are difficult to integrate on regional, continental and global scales. The results presented here show that, in spite of considerable heterogeneity in local environmental and biological parameters (Tables 2 and 3), network-scale spatial and temporal trends are clearly discernable in the δ_{er} and Δ_{er} signals from our network of forest ecosystems. Heterogeneous $\delta^{13}C$ signals observed across these sites show both the spatial and temporal extent of variations at the ecosystem-scale, and their integrated consistency with larger-scale atmospheric measurements.

The mechanism for the observed trends in δ_{er} appears to have been closely related with prevailing meteorological conditions, particularly moisture supply, on both seasonal and interannual time scales. Interannual variability is particularly significant as it often constitutes a major uncertainty in understanding ecosystem functioning (e.g. Schimel *et al.*, 1994; Randerson *et al.*, 2002b). The results both demonstrate the significance of interannual differences in δ_{er} values, and provide insights into their possible basis. In 2001, a relatively dry year, spatial (dominated by longitudinal) variations and the marginal seasonal cycle in δ_{er} were more significantly correlated with atmospheric water content (RH and VPD) than T_a or P_m. Yet, in the wetter

2002, summer (July–August) δ_{er} values were significantly related with T_a and P_m, but not with RH or VPD. As the relationship between δ_{er} and P_m was inverse to that expected, it is likely that this correlation is secondary, as a result of the significant relationship between T_a and P_m ($R^2 = 0.45$, results not shown). The main environmental differences between these 2 years were in the amount and seasonal distribution of precipitation. During 2001, total precipitation in the July–October period was focused in September–October, but in 2002, most sites experienced considerably enhanced precipitation during the period of peak activity in August (which also caused large-scale flooding in eastern Europe). Such responses would be expected as different limiting factors, i.e. atmospheric humidity and soil water supply, vary in their influence on plant activity (cf. Fritts, 1976). This has been demonstrated clearly through the relatively extreme seasonal cycle at the semi-arid Yatir forest site (Israel), where soil respiration is highly correlated with temperature only during the wet winter period, and with soil water content only during the dry summer period (Grünzweig JM, Hemming DL, Lin T, unpublished results).

The strong association noted between δ_{er} and daytime average VPD and RH in 2001 is consistent with studies that associate higher VPD with lower leaf conductance and leaf-level ^{13}C discrimination and, therefore, less negative $\delta^{13}C$ values of recently formed photosynthates, and *vice versa* (Farquhar *et al*., 1982; Brugnoli *et al*., 1988; Collatz *et al*., 1991). This indicates that autotrophic respiration (which carries this signal) and its dynamics were important influences on δ_{er} values in 2001. This is also supported by the pronounced longitudinal variations in δ_{er} and meteorological parameters (VPD, RH and T_a) during the summer (July and August) of 2001. It is not clear why RH shows a more significant correlation with δ_{er} than VPD, although it could be explained by the fact that VPD in this study is calculated relative to T_a, which is not always representative of leaf boundary layer temperatures. In 2002, when no clear association was observed between δ_{er} and either RH or VPD, but significant relationships were noted between δ_{er} and T_a and P_m, it is possible that the influence of stomatal regulation by VPD and RH on the ^{13}C of the combined autotrophic/heterotrophic respiration flux was considerably reduced (relative to 2001), while T_a became a more dominant influence (explaining 76% of the variance in δ_{er}), as discussed above. Note that the significant positive relationship between δ_{er} and P_m in 2002 is opposite to that expected from water stress-induced stomatal regulation, and other results from forest ecosystem δ_{er} studies (e.g. Pataki *et al*., 2003). As argued above, this positive relationship is likely to be indirect as a result of the significant positive relationship between T_a and P_m during the same period.

The results discussed above highlight relationships between daytime average meteorological conditions and the corresponding night-time δ_{er} values, but it has been shown before that time-lags exist in δ_{er} response to environmental signals (Horwath *et al*., 1994; Andrews *et al*., 1999; Mikan *et al*., 2000; Ekblad & Högberg, 2001; Högberg *et al*., 2001; Bowling *et al*., 2002; Knohl *et al*., 2003; McDowell *et al*., 2004). The 0.5 h time resolution of the meteorological data used to check time-lags in our data (Fig. 9) identified a diurnal cycle in the correlations between δ_{er} and VPD, RH and T_a in 2001. As most of the significant lagged correlations in 2001 were noted between the night-time δ_{er} values and mid-day meteorological conditions on the same/preceding day, this suggests a rapid (several hours) turnover of at least part of the newly formed photosynthate. This was likely associated with the most active sinks, or those in closest proximity to the sites of production. The basis for the continued diurnal fluctuations in the correlations for up to 7 days prior to sampling is not clear. It may identify contributions from a common photosynthate pool with slower turnover rates, including photosynthate translocated to trunks and roots. Interestingly, this would also indicate some cycling in the utilization of carbon pools for respiration between day and night. The results may also reflect some periodicity and autocorrelation of environmental signals over time. Nevertheless, these results are consistent with other, specific observations at the Collelongo site, Italy, which showed that δ_{er} was significantly correlated with leaf and phloem sap $\delta^{13}C$ variations, and these were closely associated with recent (within a few days) meteorological fluctuations (Scartazza *et al*., 2004). Note, though, that our results show a network-scale response and indicate a faster isotopic signal transduction than the 5–10 days time-lags reported in most other individual forest studies, cited above. The longer or the more irregular the turnover of carbon used in respiration, the greater the expected interference and noise in the δ_{er} signal, e.g. from stored carbohydrates, heterotrophic decomposition of plant organic matter, and mixing of various photosynthate pools. Such factors may have contributed to the low lag correlations observed in 2002. Here too, this was likely enhanced by the uncharacteristically high mid-summer precipitation and potentially irregular utilization of ecosystem carbon pools during that year.

A key contribution of isotopic studies to ecosystem research is in understanding the partitioning of bulk canopy CO_2 into its source components utilizing $\delta^{13}C$ and $\delta^{18}O$ analyses (Yakir & Sternberg, 2000; Bowling *et al*., 2001b), girdling (Högberg *et al*., 2001;

Bhupinderpal-Singh *et al*., 2003) and $\delta^{14}C$ dating (Gaudinski *et al*., 2000). In this study, we examined the suitability of partitioning δ_{er} into autotrophic and heterotrophic components utilizing $\delta^{13}C$ values from leaf and soil material as surrogates for the $\delta^{13}C$ values of respired CO_2 from these components (see Methods). The results showed that this approach was not suitable for partitioning the forest δ_{er} fluxes in this study during the seasonal cycle. The possible reasons for this are many, including, (a) differences in the time periods represented by $\delta^{13}C_L$ (early season leaf growth), $\delta^{13}C_{St}$ (main season growth), $\delta^{13}C_{So}$ (differential organic matter contributions and decomposition rates) (Pataki *et al*., 2003), (b) large variations in δ_{au} that were not represented by any contribution to structural material, (c) unrepresentative $\delta^{13}C_{So}$ values at 0–5 cm depths relative to the whole soil column and the δ_h contribution (Fessenden & Ehleringer, 2002) and (d) complex dynamics regulating the contributions of present and stored carbon to organic matter formation (Hemming *et al*., 2001). Support for such inconsistencies was also noted in experiments at Collelongo, Italy, which showed large summer enrichments in $\delta^{13}C$ records from plant sugars and leaf respired CO_2 but stable organic matter $\delta^{13}C$ values throughout the seasonal cycle (Scartazza *et al*., 2004). Similarly, measurements of the diurnal and seasonal variations in the $\delta^{13}C$ of leaf respired CO_2 and leaf metabolites at Yatir forest, Israel were typically $>2.0‰$ different from the $\delta^{13}C$ of bulk leaf organic matter (Maseyk *et al*., unpublished results).

An interesting observation from the organic matter $\delta^{13}C$ results was the general enrichment observed from $\delta^{13}C_L$ to $\delta^{13}C_{St}$ to $\delta^{13}C_{Rt}$. This is consistent with similar trends observed between $\delta^{13}C_L$ and $\delta^{13}C_{Rt}$ of *Helianthus annuus* L. (Lauteri *et al*., 1993), and it may be explained by a number of factors: (a) variations in the relative proportions of chemical components in the different plant components (Schmidt & Gleixner, 1998; Jäggi *et al*., 2002), (b) progressive fractionation or preferential substrate use during respiration (Tcherkez *et al*., 2003), (c) offsets in the timing of formation of the different components (Fritts, 1976) and (d) variability in leaf or tree characteristics (Schleser & Jayasekera, 1985; Leavitt & Newberry, 1992). Likewise, the enrichment of $\delta^{13}C_{So}$ compared with $\delta^{13}C_L$ or $\delta^{13}C_{St}$ is in agreement with numerous studies (Melillo *et al*., 1989; Boutton, 1996; Buchmann *et al*., 1997; Flanagan *et al*., 1999; Ehleringer *et al*., 2000; Grünzweig *et al*., 2003), although it contrasts with depletions in $\delta^{13}C_{So}$ noted during the early phase of decomposition by Benner *et al*. (1987) and Schleser *et al*. (1999). Again, there are multiple possible explanations for these variations, including, (a) enrichment of the soil decomposer organisms relative to their carbon sources (DeNiro & Epstein, 1978; Gleixner *et al*., 1993); (b) variations in leaf and litter chemical composition or decomposition characteristics (Benner *et al*., 1987); (c) the recent trend towards more depleted atmospheric CO_2 from anthropogenic emissions, resulting in older soil carbon being relatively enriched compared with the newer substrate carbon (Quay *et al*., 1992; Tans *et al*., 1993; Fung *et al*., 1997; Ciais *et al*., 1999); (d) unrepresentative sampling of lower canopy foliage (Knohl *et al*., 2005). The fact that sites with angiosperm species exhibit more significant average enrichments between $\delta^{13}C_L$ and $\delta^{13}C_{So}$ than gymnosperm suggests that the particular chemical and/or soil decomposition characteristics of these species may contribute to this offset. Similarly, other species-specific characteristics, like environmental tolerance, phenology and growth dynamics could also influence the specific plant and soil $\delta^{13}C$ values (Schleser, 1985; Leavitt & Newberry, 1992; Hemming *et al*., 1998). Further studies are clearly required to establish the reasons for these differences. Nevertheless, even on a preliminary basis, the results indicate that isotopic fractionation during respiration could account for the observed effects, and it should not be expected that the $\delta^{13}C$ of respired CO_2 is well represented by the bulk organic material sampled (i.e. soil, stem or leaf). As we examined the $\delta^{13}C$ of bulk soil organic carbon, rather than the substrate for heterotrophic respiration, this could not be examined further here.

One of the key motivations for establishing the isotope network was to examine the nature of scaling between ecosystem- and regional-scale $\delta^{13}C$ data. It is known that CO_2 exchanges by the terrestrial biosphere dominate the observed seasonal cycles of atmospheric $[CO_2]$ and $\delta^{13}C$ at background air monitoring stations (see Introduction), and it is also generally accepted that forest ecosystems account for a significant portion of those CO_2 exchanges (IPCC, 2001). However, the linkages between ecosystem- and regional-scales are not well understood. We compared our network δ_{er} and Δ_{er} signals with regional-scale $\delta^{13}C$ signatures (see Methods) to examine the consistency between scales. A precise match was not anticipated because background air integrates more CO_2 sources and sinks than those represented by our network sites. Nevertheless, the close relationship between the $\delta^{13}C$ signals at these two scales observed during the summer and autumn of 2001 suggested that our forest CO_2 fluxes were rather representative of the larger-scale fluxes over this region. Furthermore, the good match between the NOAA/CMDL daytime sampling with the network night-time sampling further indicated close links between the photosynthetic (daytime) and respiration (night-time) isotopic signals (see Introduction). Note, however, that the estimates of δ_{er} and regional-scale $\delta^{13}C$ signatures

can be influenced by contributions, sinks and sources, other than from forest ecosystems, including anthropogenic, that may significantly influence air samples, particularly outside the dominant growth season (Bakwin *et al*., 1998; Florkowski *et al*., 1998; Potosnak *et al*., 1999; Takahashi *et al*., 2001; Demény & Haszpra, 2002). Such effects could have been a significant influence, for example, on the observed ^{13}C depletion at both the regional- and ecosystem-level in late October and November, although, it should be remembered that even lower $\delta^{13}C$ values were observed for organic matter components (especially leaves) at some of the forest sites. In 2002, regional background $\delta^{13}C$ signatures from central Europe, although still within range, did not capture the depleted δ_{er} signal of that year, showing a value significantly enriched compared with both our forest δ_{er} signals and the regional signature from north-western Europe. While the forests' depleted δ_{er} signal seems robust across the network and sampling times, and consistent with that year's meteorology, the background sampling at Hungary may have been influenced by relatively local signals. Indeed, the large error of this estimate, particularly for the summer period, and the unexpectedly large difference between the two background regional values during autumn, are consistent with nonforest ecosystem CO_2 fluxes and ^{13}C signals at the Hegyhatsal site. More analyses of the seasonal $\delta^{13}C$ and CO_2 data from Hegyhatsal is required to substantiate this.

Inverse models, that partition atmospheric CO_2 changes into their component oceanic and terrestrial sources and sinks, typically utilize estimated 'discrimination' values, Δ, to parameterize the terrestrial ecosystem signal (Eqn (1)). The advantage of using Δ is that it is independent of standard materials (see definition of δ in Introduction) and accounts for existing variations in δ_a values (e.g. Fig. 3). However, when δ_a is not known *a priori* the use of Δ requires consideration. In some cases, fluctuations in δ_a were assumed to be minor over large spatial and temporal ranges, and a mean $\delta^{13}C$ of 'background' air was used (Buchmann *et al*., 2002; Lai *et al*., 2004). Results presented here, however, demonstrate that Δ_{er} could vary by up to 2.2‰ depending on the method used to estimate δ_a. Furthermore, a recent study by Hurwitz *et al*. (2004) indicates that the 5-day average mixing ratio of CO_2 can vary by up to 10 ppm over several days, demonstrating the possible significance of δ_a in an estimation of Δ.

Of the three methods for estimating δ_a compared in this study, Methods 1 and 2 were intrinsically linked with the slope method equations, and therefore, inaccuracies in the regression line fits could have induced errors in the δ_a estimate. If this were the case, the maximum differences in δ_a between methods, between mid-July and -September, would be expected to coincide with the largest SEs in our δ_{er} estimates (Table 3). However, during this period SEs were typically at their lowest (<1.0‰). Alternatively, it is more likely that the main differences in δ_a occur because the methods estimate δ_a for very different spatial scales; Method 3 relates to δ_a relatively high in the mixed planetary boundary layer, while Methods 1 and 2 relate more intimately to the canopy boundary layer, which is closely linked with ecosystem activity. All methods have possible inaccuracies and it is not clear which is more 'correct' for estimating δ_a. Using Methods 1 and 2 has the advantage that the δ_a values would be closely coupled with the atmospheric CO_2 in contact with ecosystem canopies, and they necessarily lay on the Keeling plot regression line (but would also be prone to rapid variability not always adequately captured by periodic sampling). In comparison, δ_a values estimated using Method 3 would be much less variable, but they would not necessarily lie along the ecosystem Keeling plot regression line, violating, in those cases, the assumption of the two end member mixing model (Eqn (3)). Nevertheless, Method 3 values would have the general advantage that ultimately, for inverse modeling we are interested in the ecosystem isotopic forcing with regard to the regional atmosphere. It could be concluded that the differences noted between δ_a estimates indicate that it may be preferable to employ directly δ_{er} (as well as δ_{ph}) values in atmospheric budget calculations, especially when these are measured at the relevant scale for the calculation.

Despite the possible uncertainties in the estimation of δ_a and δ_{er}, Δ_{er} estimates calculated in this study are in general agreement within the broad range of C_3 plant and 'ecosystem discrimination' reported in other studies (cf. Buchmann & Kaplan, 2001 and references therein), although, the wide range of values, approaches and methodologies used makes a more detailed comparison difficult. As the variability in δ_{er} is almost directly translated to Δ_{er} (Eqn (2)), because δ_a changes are usually relatively small, trends and relationships observed with the δ_{er} values also generally apply to Δ_{er}. A major highlight of these results is that, as for δ_{er}, the summer offset in average Δ_{er} between years, and the seasonal and spatial trends during the main growth periods were significantly related to prevailing meteorological variations. Notably, variations in Δ_{er} of the magnitude observed here could induce, at the global scale, annual net atmosphere–biosphere flux estimates from inverse models to vary significantly (Randerson *et al*., 2002b). Scholze *et al*. (2003) estimated that such variations could alter

terrestrial biospheric flux estimates by $\sim 0.5\,\mathrm{PgC\,yr^{-1}}$, which can be as large as $\sim 25\%$ of their mean annual sink. The observed general robustness of δ_{er} and Δ_{er} values at high NEE may simplify the treatment of seasonal changes in these variables in models.

Conclusions

Using a 'Keeling plot' type approach, we have shown that a simple, low cost canopy air sampling program can provide estimates of δ_{er} values on ecosystem to continental scales. Accounting for variations in δ_a by deriving Δ_{er} estimates highlighted important considerations and limitations for Δ_{er} estimates which are often used in global atmospheric budgets. Despite considerable differences in site and species characteristics across the network, we demonstrated that coherent space- and time-dependent trends can be discernable, and significant relationships observed between δ_{er}, Δ_{er} and meteorological conditions. The most significant time-lags in the δ_{er} vs. meteorological relationships were shorter than reported in other studies, indicating the possible dynamics involved in this signal transduction.

Comparing δ_{er} results with the $\delta^{13}C$ values of organic matter in leaves, stems and soil clearly showed that short term δ_{er} values cannot be partitioned into autotrophic and heterotrophic components using organic matter $\delta^{13}C$ data as constraints. The organic matter $\delta^{13}C$ results, nevertheless, highlighted the possibility of ^{13}C fractionation during respiration as reflected in progressive ^{13}C enrichment from leaves, through stems and roots to soil organic matter.

A generally good agreement between ecosystem- and regional-scale atmospheric observations was obtained in this study, suggesting that regional-scale atmospheric sampling programs generally, but not always, capture well the dominant forest ecosystem $\delta^{13}C$ signatures in Europe. Our network estimate of mean δ_{er} and Δ_{er} values were -25.6 ± 1.9‰ and 17.8 ± 2.0‰ in 2001 and -26.6 ± 1.5‰ and 19.0 ± 1.6‰ in 2002. Such variations between years were largely explained by climatic influences (particularly precipitation amount and its seasonal distribution) on ecophysiological processes, which where not well captured in the regional estimates but are important to consider in inverse models to improve terrestrial carbon flux estimates. These data constitute a valuable resource for validation and improved parameterization of large-scale terrestrial ecosystem models.

Acknowledgements

D. H. and D. Y. gratefully acknowledge Emanuela Negreanu for her technical expertise and help with all the $\delta^{13}C$ analyses, and R. Benmair, J. Grünzweig, K. Maseyk, E. Rotenberg, H. Sagi and A. Planer for assistance with various aspects of this research. D. H. and D. Y. acknowledge the financial support provided through the European Community's Human Potential Programme under contract HPRN-CT-1999-00059, NETCARB. D. Y. also gratefully acknowledges funding for various parts of this project from EU (Carboeuroflux, EVK2-CT-1999-00032); GLOWA-JR (01-02-01752); ISF 695/99); BSF (2000293); IALC (04-DG-1132403-019); Minerva-Avron Photosynthesis Centre. B. O. and K. B. acknowledge the support of the Council for Forest Research Development (COFORD), Ireland for funding (site in Dooary). B. K. and T. G. gratefully acknowledge the support of CARBOEUROFLUX (EU, EVK2-CT-1999-0032) and VERTIKO (Federal Ministry for Education and Research, Germany, PT UKF 07ATF37) at the Tharandt site.

References

Andres RJ, Fielding DJ, Marland G *et al*. (1999) Carbon dioxide emissions from fossil-fuel use, 1751–1950. *Tellus B*, **51**, 759–765.

Andres RJ, Marland G, Fung I *et al*. (1996) A $1^\circ \times 1^\circ$ distribution of carbon dioxide emissions from fossil fuel consumption and cement manufacture, 1950–1990. *Global Biogeochemical Cycles*, **10**, 419–429.

Andrews JA, Harrison KG, Matamala R *et al*. (1999) Separation of root respiration from total soil respiration using carbon-13 labeling during free-air carbon dioxide enrichment (FACE). *Soil Science Society of America Journal*, **63**, 1429–1435.

Aubinet M, Grelle A, Ibrom A *et al*. (2000) Estimates of the annual net carbon and water exchange of forests: the EUROFLUX methodology. *Advances in Ecological Research*, **30**, 113–175.

Bakwin PS, Tans PP, White JWC *et al*. (1998) Determination of the isotopic ($^{13}C/^{12}C$) discrimination by terrestrial biology from a global network of observations. *Global Biogeochemical Cycles*, **12**, 555–562.

Bakwin PS, Tans PP, Zhao CL *et al*. (1995) Measurements of carbon-dioxide on a very tall tower. *Tellus B*, **47**, 535–549.

Battle M, Bender ML, Tans PP *et al*. (2000) Global carbon sinks and their variability inferred from atmospheric O-2 and delta C-13. *Science*, **287**, 2467–2470.

Benner R, Fogel ML, Sprague EK *et al*. (1987) Depletion of C-13 in lignin and its implications for stable carbon isotope studies. *Nature*, **329**, 708–710.

Bhupinderpal-Singh A, Nordgren A, Lofvenius MO *et al*. (2003) Tree root and soil heterotrophic respiration as revealed by girdling of boreal Scots pine forest: extending observations beyond the first year. *Plant, Cell and Environment*, **26**, 1287–1296.

Bousquet P, Peylin P, Ciais P *et al*. (2000) Regional changes of CO_2 fluxes over land and oceans since 1980. *Science*, **290**, 1342–1346.

Boutton TW (1996) Stable carbon isotope ratios of soil organic matter and their use as indicators of vegetation and climate change. In: *Mass Spectrometry of Soils* (eds Boutton TW, Yamasaki S), pp. 47–82. Marcel Dekker Inc, New York, NY, USA.

Bowling DR, Cook CS, Ehleringer JR (2001a) Techniques to measure CO_2 mixing ratio in small flasks with a bellows/IRGA system. *Agricultural and Forest Meteorology*, **109**, 61–65.

Bowling DR, McDowell NG, Bond BJ *et al*. (2002) ^{13}C content of ecosystem respiration is linked to precipitation and vapor pressure deficit. *Oecologia*, **131**, 113–124.

Bowling DR, Tans PP, Monson RK (2001b) Partitioning net ecosystem carbon exchange with isotopic fluxes of CO_2. *Global Change Biology*, **7**, 127–145.

Broecker WS, Ledwell JR, Takahashi T *et al*. (1986) Isotopic versus micrometeorological ocean CO_2 fluxes: a serious conflict. *Journal of Geophysical Research*, **91**, 10,517–10,527.

Brugnoli E, Hubick KT, von Caemmerer S *et al*. (1988) Correlation between the carbon isotope discrimination in leaf starch and sugars of C3 plants and the ratio of intercellular and atmospheric partial pressure of carbon dioxide. *Plant Physiology*, **88**, 1418–1424.

Buchmann N, Brooks JR, Ehleringer JR (2002) Predicting daytime carbon isotope ratios of atmospheric CO_2 within forest canopies. *Functional Ecology*, **16**, 49–57.

Buchmann N, Kao WY, Ehleringer JR (1997) Influence of stand structure on carbon-13 of vegetation, soils, and canopy air within deciduous and evergreen forests in Utah, United States. *Oecologia (Berlin)*, **110**, 109–119.

Buchmann N, Kaplan JO (2001) Carbon isotope discrimination of terrestrial ecosystems – How well do observed and modeled results match? In: *Global Biogeochemical Cycles in the Climate System* (eds Schulze ED, Heimann M, Harrison S, Holland E, Lloyd J, Prentice IC, Schimel DS), pp. 253–266. Academic Press, New York, NY, USA.

Ciais P, Friedlingstein P, Schimel DS *et al*. (1999) A global calculation of the delta C-13 of soil respired carbon: implications for the biospheric uptake of anthropogenic CO_2. *Global Biogeochemical Cycles*, **13**, 519–530.

Ciais P, Tans PP, White JWC *et al*. (1995) Partitioning of ocean and land uptake of CO_2 as inferred by $\delta^{13}C$ measurements from the NOAA Climate Monitoring and Diagnostics Laboratory Global Air Sampling Network. *Journal of Geophysical Research*, **100**, 5051–5070.

Collatz JG, Ball TJ, Grivet C *et al*. (1991) Physiological and environmental regulation of stomatal conductance, photosynthesis and transpiration: a model that includes a laminar boundary layer. *Agricultural and Forest Meteorology*, **54**, 107–136.

Conway TJ, Tans PP, Waterman LS *et al*. (1994) Evidence for interannual variability of the carbon-cycle from the National Oceanic and Atmospheric Administration Climate Monitoring and Diagnostics Laboratory Global Air Sampling Network. *Journal of Geophysical Research-Atmospheres*, **99**, 22,831–22,855.

Coplen TB (1994) Reporting of stable hydrogen, carbon, and oxygen isotopic abundances. *Pure and Applied Chemistry*, **66**, 273–276.

Demény A, Haszpra L (2002) Stable isotope compositions of CO_2 in background air and at polluted sites in Hungary. *Rapid Communications in Mass Spectrometry*, **16**, 797–804.

DeNiro MJ, Epstein S (1978) Influence of diet on the distribution of carbon isotopes in animals. *Geochimica et Cosmochimica Acta*, **42**, 495–506.

Ehleringer JR, Buchmann N, Flanagan LB (2000) Interpreting belowground processes using carbon and oxygen isotope ratios. *Ecological Applications*, **10**, 412–422.

Ehleringer JR, Cerling TE (1995) Atmospheric CO_2 and the ratio of intercellular to ambient CO_2 concentrations in plants. *Tree Physiology*, **15**, 105–111.

Ehleringer JR, Cerling TE, Helliker BR (1997) C_4 photosynthesis, atmospheric CO_2, and climate. *Oecologia (Berlin)*, **112**, 285–299.

Ekblad A, Högberg P (2001) Natural abundance of ^{13}C in CO_2 respired from forest soils reveals speed of link between tree photosynthesis and root respiration. *Oecologia*, **127**, 305–308.

Enting IG, Trudinger CM, Francey RJ (1995) A synthesis inversion of the concentration and $\delta^{13}C$ of atmospheric CO_2. *Tellus*, **47B**, 35–52.

Farquhar GD, Ehleringer JR, Hubick KT (1989) Carbon isotope discrimination and photosynthesis. *Annual Reviews of Plant Physiology and Plant Molecular Biology*, **40**, 503–537.

Farquhar GD, O'Leary MH, Berry JA (1982) On the relationship between carbon isotope discrimination and intercellular carbon dioxide concentration in leaves. *Australian Journal of Plant Physiology*, **9**, 121–137.

Fessenden JE, Ehleringer JR (2002) Age-dependent variations in $\delta^{13}C$ of ecosystem respiration across a coniferous forest chronosequence in the Pacific Northwest. *Tree Physiology*, **22**, 159–167.

Flanagan LB, Kubien DS, Ehleringer JR (1999) Spatial and temporal variation in the carbon and oxygen stable isotope ratio of respired CO_2 in a boreal forest ecosystem. *Tellus*, **51B**, 367–384.

Florkowski T, Korus A, Miroslaw J *et al*. (1998) Isotopic composition of CO_2 and CH_4 in a heavily polluted urban atmosphere and in a remote mountain area (Southern Poland). In: *Isotope Techniques in the Study of Environmental Change*, pp. 37–48. IAEA, Vienna, Austria.

Fritts HC (1976) *Tree Rings and Climate*. Academic Press Inc., New York, NY, USA.

Fung I, Field CB, Berry JA *et al*. (1997) Carbon-13 exchanges between the atmosphere and biosphere. *Global Biogeochemical Cycles*, **11**, 507–533.

Gaudinski JB, Trumbore SE, Davidson EA *et al*. (2000) Soil carbon cycling in a temperate forest: radiocarbon-based estimates of residence times, sequestration rates and partitioning of fluxes. *Biogeochemistry*, **52**, 113–114.

Gleixner G, Danier H-J, Werner RA *et al*. (1993) Correlations between the ^{13}C content of primary and secondary plant products in different cell compartments and that in decomposing basidiomycetes. *Plant Physiology*, **102**, 1287–1290.

Gloor M, Bakwin P, Hurst D *et al*. (2001) What is the concentration footprint of a tall tower? *Journal of Geophysical Research-Atmospheres*, **106**, 17831–17840.

Grünzweig JM, Sparrow SD, Chapin FS (2003) Impact of forest conversion to agriculture on carbon and nitrogen mineralization in subarctic Alaska. *Biogeochemistry*, **64**, 271–296.

Hemming D, Fritts HC, Leavitt SW *et al*. (2001) Modelling tree-ring $\delta^{13}C$. *Dendrochronologia*, **19**, 23–38.

Hemming DL, Switsur VR, Waterhouse JS *et al*. (1998) Climate variation and the stable carbon isotope composition of tree ring cellulose: an intercomparison of *Quercus robur*, *Fagus sylvatica* and *Pinus silvestris*. *Tellus*, **50B**, 25–33.

Högberg P, Nordgren A, Buchmann N *et al*. (2001) Large-scale forest girdling shows that current photosynthesis drives soil respiration. *Nature*, **411**, 789–792.

Horwath WR, Pretziger KS, Paul EA (1994) ^{14}C allocation in tree–soil systems. *Tree Physiology*, **19**, 1163–1176.

Hurwitz MD, Ricciuto DM, Bakwin PS *et al*. (2004) Transport of carbon dioxide in the presence of storm systems over a Northern Wisconsin forest. *Journal of the Atmospheric Sciences*, **61**, 607–618.

Inoue H, Sugimura Y (1985) Carbon isotopic fractionation during the exchange process between air and sea water under equilibrium and kinetic conditions. *Geochimica et Cosmochimica Acta*, **49**, 2453–2460.

IPCC (2001) *Climate Change: The Scientific Basis*. Cambridge University Press, Cambridge, UK.

Jäggi M, Saurer M, Fuhrer J *et al*. (2002) The relationship between the stable carbon isotope composition of needle bulk material, starch, and tree rings in *Picea abies*. *Oecologia*, **131**, 325–332.

Keeling CD (1958) The concentration and isotopic abundances of atmospheric carbon dioxide in rural areas. *Geochimica et Cosmochimica Acta*, **13**, 322–334.

Keeling CD (1961) The concentration and isotopic abundances of carbon dioxide in rural and marine air. *Geochimica et Cosmochimica Acta*, **24**, 277–298.

Knohl A, Schumacher M, Söe A *et al*. (2003) SPA^{13}CE – Short term variability of the ^{13}C signal at various ecosystem scales. *Abstracts of the CarboEurope Conference The continental carbon cycle* 19–21 March, Lisbon, Portugal.

Knohl A, Werner RA, Brand WA *et al*. (2005) Short-term variations in $\delta^{13}C$ of ecosystem respiration reveals link between assimilation and respiration in a deciduous forest. *Oecologia*, **142**, 70–82.

Lai CT, Ehleringer JR, Tans P *et al*. (2004) Estimating photosynthetic C-13 discrimination in terrestrial CO_2 exchange from canopy to regional scales. *Global Biogeochemical Cycles*, **18**, Art. No. GB1041, doi: 10.1029/2003GB002148.

Lauteri M, Brugnoli E, Spaccino L (1993) Carbon isotope discrimination in leaf soluble sugars and in whole plant dry matter in *Helianthus annuus* L. grown under different water conditions. In: *Stable Isotopes and Plant Carbon–Water Relations* (eds Ehleringer JR, Hall AE, Farquhar GD), pp. 93–108. Academic Press Inc., London.

Leavitt SW, Newberry T (1992) Systematics of stable-carbon isotopic differences between gymnosperm and angiosperm trees. *Plant Physiology*, **11**, 257–262.

Levin I, Ciais P, Langenfelds R *et al*. (2002) Three years of trace gas observations over the EuroSiberian domain derived from aircraft sampling – a concerted action. *Tellus B*, **54**, 696–712.

Levin I, Kromer B, Schmidt M *et al*. (2003) A novel approach for independent budgeting of fossil fuel CO_2 over Europe by (CO_2)-C-14 observations. *Geophysical Research Letters*, **30**, 2194.

Lindner M, Lasch P, Cramer W (1996) Application of a forest succession model to a continentality gradient through Central Europe. *Climatic Change*, **34**, 191–199.

Lloyd J, Farquhar GD (1994) ^{13}C discrimination by the terrestrial biosphere. *Oecologia*, **99**, 201–215.

Loader NJ, Switsur VR, Field EM (1995) High-resolution stable isotope analysis of tree rings: implications of 'microdendroclimatology' for palaeoenvironmental research. *Holocene*, **5**, 457–460.

Maksyutov S, Machida T, Mukai H *et al*. (2003) Effect of recent observations on Asian CO_2 flux estimates by transport model inversions. *Tellus B*, **55**, 522–529.

Marland G, Boden TA, Andres RJ (2003) Global, regional, and national CO_2 emissions. In *Trends: A Compendium of Data on Global Change*. Carbon Dioxide Information Analysis Center, Oak Ridge National Laboratory, U.S. Department of Energy, Oak Ridge, TN, USA.

McDowell NG, Bowling DR, Bond BJ *et al*. (2004) Response of the carbon isotopic content of ecosystem, leaf, and soil respiration to meteorological and physiological driving factors in a *Pinus ponderosa* ecosystem. *Global Biogeochemical Cycles*, **18**, Art. No. GB1013, doi: 10.1029/2003GB002049.

Melillo JM, Aber JD, Linkins AE (1989) Carbon and nitrogen dynamics along the decay continuum: plant litter to soil organic matter. In: *Ecology of Arable Land* (eds Clarholm M, Bergström L), pp. 53–62. Kluwer Academic Publishers, Dordrecht.

Mikan CJ, Zak DR, Kubiske ME *et al*. (2000) Combined effects of atmospheric CO_2 and N availability on the below-ground carbon and nitrogen dynamics of aspen mesocosms. *Oecologia*, **124**, 432–445.

Miller JB, Tans PP (2003) Calculating isotopic fractionation from atmospheric measurements at various scales. *Tellus B*, **55**, 207–214.

Miller JB, Tans PP, White JWC *et al*. (2003) The atmospheric signal of terrestrial carbon isotopic discrimination and its implications for partitioning carbon fluxes. *Tellus B*, **55**, 197–206.

Nakazawa T, Morimoto S, Aoki S *et al*. (1993) Time and space variations of the carbon isotopic ratio of tropospheric carbon dioxide over Japan. *Tellus B*, **45**, 258–274.

Nakazawa T, Morimoto S, Aoki S *et al*. (1997) Temporal and spatial variations of the carbon isotopic ratio of atmospheric carbon dioxide in the western Pacific region. *Journal of Geophysical Research-Atmospheres*, **102**, 1271–1285.

Ogee J, Peylin P, Cuntz M *et al*. (2004) Partitioning net ecosystem carbon exchange into net assimilation and respiration with canopy-scale isotopic measurements: an error propagation analysis with (CO_2)-C-13 and (COO)-O-18 data. *Global Biogeochemical Cycles*, **18**, GB2019, doi: 10.1029/2003GB002166.

Oliver JE, Fairbridge RW (1987) *The Encyclopedia of Climatology*, *Encyclopedia of Earth Sciences*, **Vol. 11**. Van Nostrand Reinhold Company Inc., New York, NY, USA.

Pataki DE, Ehleringer JR, Flanagan LB *et al*. (2003) The application and interpretation of Keeling plots in terrestrial carbon cycle research. *Global Biogeochemical Cycles*, **17**, 1022.

Potosnak MJ, Wofsy SC, Denning AS *et al*. (1999) Influence of biotic exchange and combustion sources on atmospheric CO_2 concentration in New England from observations at a forest flux tower. *Journal of Geophysical Research*, **104**, 9561–9569.

Quay PD, Tilbrook B, Wong CS (1992) Oceanic uptake of fossil-fuel CO_2-^{13}C evidence. *Science*, **256**, 74–79.

Randerson JT, Collatz GJ, Fessenden JE *et al*. (2002b) A possible global covariance between terrestrial gross primary production and C-13 discrimination: consequences for the atmospheric C-13 budget and its response to ENSO. *Global Biogeochemical Cycles*, **16**, 83-1–83-16.

Randerson JT, Enting IG, Schuur EAG *et al*. (2002a) Seasonal and latitudinal variability of troposphere $\delta(CO_2)$-C-14: post bomb contri-

butions from fossil fuels, oceans, the stratosphere, and the terrestrial biosphere. *Global Biogeochemical Cycles*, **16**, 59-1–59-19.

Robertson I, Switsur VR, Carter AHC *et al*. (1997) Signal strength and climate relationships in $^{13}C/^{12}C$ ratios of tree ring cellulose from oak in east England. *Journal of Geophysical Research*, **102**, 19,507–19,516.

Saurer M, Siegenthaler U (1989) $^{13}C/^{12}C$ isotope ratios in trees are sensitive to relative humidity. *Dendrochronologia*, **7**, 9–13.

Scartazza A, Mata C, Matteucci G *et al*. (2004) Comparisons of $\delta^{13}C$ of photosynthetic products and of ecosystem respiratory CO_2 and their responses to seasonal climate variability. *Oecologia*, **140**, 340–351.

Schimel DS, Braswell BH, Holland EA *et al*. (1994) Climatic, edaphic and biotic controls over storage and turnover of carbon in soils. *Global Biogeochemical Cycles*, **8**, 279–293.

Schleser GH (1985) Parameters determining carbon isotope ratios in plants. In: *Proceedings of the Workshop: Modelling of Tree-Ring Development – Cell Structure and Environment, Freiburg, September 5–9th* (eds Spiecker H, Kahle) P. Institut fur Waldwafhstuh, Universitat Freiburg, Germany.

Schleser GH, Frielingsdorf J, Blair A (1999) Carbon isotope behaviour in wood and cellulose during artificial aging. *Chemical Geology*, **158**, 121–130.

Schleser GH, Jayasekera R (1985) $\delta^{13}C$-variations of leaves in forests as an indication of reassimilated CO_2 from the soil. *Oecologia*, **65**, 536–542.

Schmidt H-L, Gleixner G (1998) Carbon isotope effects on key reactions in plant metabolism and ^{13}C-patterns in natural compounds. In: *Stable Isotopes* (ed. Griffiths H), pp. 13–25. BIOS Scientific Publishers Ltd, Oxford, UK.

Scholze M, Kaplan JO, Knorr W *et al*. (2003) Climate and interannual variability of the atmosphere–biosphere $^{13}CO_2$ flux. *Geophysical Research Letters*, **30**, 69(1–4), doi: 10.1029/2002EL015631.

Sokal RR, Rholf FJ (1995) *Biometry: The Principles and Practice of Statistics in Biological Research*. Freeman, New York.

Still CJ, Berry JA, Ribas-Carbo M *et al*. (2003) The contribution of C3 and C4 plants to the carbon cycle of a tallgrass prarie: an isotopic approach. *Oecologia*, **136**, 347–359.

Swanson RV, Flanagan LB (2001) Environmental regulation of carbon dioxide exchange at the forest floor in a boreal black spruce ecosystem. *Agricultural and Forest Meteorology*, **108**, 165–181.

Switsur VR, Waterhouse JS (1998) Stable isotopes in tree ring cellulose. In: *Stable Isotopes: Integration of Biological, Ecological and Geochemical Processes* (ed. Griffiths H), pp. 303–316. Bios Scientific Publishers, Oxford, UK.

Takahashi HA, Hiyama T, Konohira E *et al*. (2001) Balance and behavior of carbon dioxide at an urban forest inferred from the isotopic and meteorological approaches. *Radiocarbon*, **43**, 659–669.

Tans P, Berry JA, Keeling RF (1993) Oceanic ^{13}C data: a new window on CO_2 uptake by the oceans. *Global Biogeochemical Cycles*, **7**, 353–368.

Tans PP, Bakwin PS, Guenther DW (1996) A feasible global carbon cycle observing system: a plan to decipher today's carbon cycle based on observations. *Global Change Biology*, **2**, 309–318.

Tans PP, Conway TJ, Nakazawa T (1989) Latitudinal distribution of the sources and sinks of atmospheric carbon dioxide derived from surface observations and atmospheric transport models. *Journal of Geophysical Research*, **94**, 5151–5172.

Tcherkez G, Nogues S, Bleton J *et al*. (2003) Metabolic origin of carbon isotope composition of leaf dark-respired CO_2 in French Bean. *Plant Physiology*, **131**, 237–244.

Trolier M, White JWC, Tans PP (1996) Monitoring the isotopic composition of atmospheric CO_2: measurements from NOAA global air sampling network. *Journal of Geophysical Research*, **101**, 25,897–25,916.

Valentini R. (ed.) (2003) Fluxes of carbon, water and energy of European forests. *Ecological Studies*, **163**, 270.

van der Werf GR, Randerson JT, Collatz GJ *et al*. (2004) Continental-scale partitioning of fire emissions during the 1997 to 2001 El Nino/La Nina period. *Science*, **303**, 73–76.

Yakir D, Sternberg LDL (2000) The use of stable isotopes to study ecosystem gas exchange. *Oecologia*, **123**, 297–311.

Yakir D, Wang XF (1996) Fluxes of CO_2 and water between terrestrial vegetation and the atmosphere estimated from isotope measurements. *Nature*, **380**, 515–517.